Expression and Localization of the PabPrx86 Peroxidase from Norway Spruce (*Picea abies* (L.) Karst.) in Tobacco (*Nicotiana benthamiana* L.)

Steven Taniwan

Master's Thesis

Master's Programme in Agricultural Sciences

emPLANT

University of Helsinki

Department of Agricultural Sciences

May 2020

HELSINGIN YLIOPISTO
HELSINGFORS UNIVERSITET
UNIVERSITY OF HELSINKI

Abstract

Tiedekunta – Fakultet – Faculty	Koulutusohjelma – Utbildningsprogram – Degree Programme
Faculty of Agriculture and Forestry	Master's Programme in Agricultural Sciences

Tekijä – Författare – Author
Steven Taniwan

Työn nimi – Arbetets titel – Title
Expression and Localization of the PabPrx86 Peroxidase from Norway Spruce (*Picea abies* (L.) Karst.) in Tobacco (*Nicotiana benthamiana* L.)

Oppiaine/Opintosuunta – Läroämne/Studieinriktning – Subject/Study track
emPLANT

Työn laji – Arbetets art – Level	Aika – Datum – Month and year	Sivumäärä – Sidoantal – Number of pages
MSc Thesis	May 2020	42

Tiivistelmä – Referat – Abstract
Norway spruce is commonly cultivated throughout Europe, Russia, and Japan. Cultivation of Norway spruce often faces the issue of fungal diseases, one of which is cherry rust disease caused by *Thekopsora areolata*. The gene model MA_10g0010 encoding an uncharacterized peroxidase (PabPrx86) has previously been associated with the presence of this pathogen. The aim of this study was to describe and assay the protein produced from this gene model, observe its localization in the cell, and determine its relative expression level in different tissues of Norway spruce. Experiments were performed by isolating the full length cDNA for *PabPrx86* and cloning the cDNA into destination vectors pEAQ-HT-DEST1 and pK7FWG2 leading to a hypertranslatable transcript and a C-terminal GFP fusion, respectively. The plasmid constructs were transformed to *Agrobacterium tumefaciens* and agro-infiltrated to *Nicotiana benthamiana*. In addition, the relative expression level of this gene in different spruce tissues at different times of the year was determined using the qRT-PCR method. Sequencing showed that there were two allelic variants of this gene in the spruce individual sampled for RNA. Results showed that both alleles code for a peroxidase with basic pI. Subcellular localization with the GFP tag detected that PabPrx86 protein was located out of cytoplasm, indicating that the protein was translated in the ER-ribosomes, whereas relative expression level analysis revealed that *PabPrx86* was highest expressed in the bud and lateral bud in June. Peroxidases are known to relate with plant defense, but further experiments are required to determine the role of *PabPrx86* in Norway spruce and what the association with *T. areolata* means.

Avainsanat – Nyckelord – Keywords
Norway spruce, PabPrx86, peroxidase

Ohjaaja tai ohjaajat – Handledare – Supervisor or supervisors
Professor Teemu Teeri

Säilytyspaikka – Förvaringsställe – Where deposited
HELDA - Helsingin yliopiston digitaalinen arkisto / HELDA - Helsingfors universitets digitala publikationsarkiv /HELDA - Digital Repository of the University of Helsinki

Muita tietoja – Övriga uppgifter – Additional information

Table of Contents

Abstract 2
Table of Contents 3
Abbreviations 4
1. Introduction 5
2. Literature Review 7
  2.1. Norway spruce 7
  2.2. Defense response 8
  2.3. Peroxidases 9
    2.3.1. Classification 9
    2.3.2. Class III peroxidases 10
3. Objectives 12
4. Materials and Methods 13
  4.1. Sample collection 13
  4.2. RNA extraction and isolation of full length cDNA for *PabPrx86* 13
  4.3. Gateway cloning of *PabPrx86* and transformation to *Escherichia coli* DH5α 15
  4.4. Transformation to *Agrobacterium* and expression in tobacco 16
  4.5. Enzymatic assays 17
    4.5.1. Protein extraction 17
    4.5.2. Activity staining and SDS-polyacrylamide gel electrophoresis (SDS-PAGE) 17
    4.5.3. Isoelectric focusing 17
  4.6. Localization of PabPrx86 18
    4.6.1. PCR reaction and Gateway cloning 18
    4.6.2. Transformation to *Agrobacterium* and visualization of PabPrx86 protein 18
  4.7. Relative expression level of *PabPrx86* in different Norway spruce tissues 19
5. Results 21
  5.1. Cloning and sequencing of full length *PabPrx86* cDNA 21
  5.2. Protein yields 22
  5.3. Sub-cellular localization of the protein from PabPrx86 28
  5.4. Relative expression level of *PabPrx86* 30
6. Discussion 31
7. Conclusion 35
Acknowledgements 36
8. References 37

Abbreviations

APX	Ascorbate Peroxidase
bp	base pairs
BSA	Bovine Serum Albumin
CP	Catalase Peroxidases
CCP	Cytochrome *c* Peroxidase
DAB	3,3'-diaminobenzidine
DAMP	Damage Associated Molecular Pattern
DAPI	4′,6-diamidino-2-phenylindole
ELISA	Enzyme-Linked Immunosorbent Assay
EPO	Eosinophil Peroxidase
EtBr	Ethidium Bromide
ER	Endoplasmic Reticulum
ETI	Effector-Triggered Immunity
ETS	Effector-Triggered Susceptibility
GFP	Green Fluorescence Protein
GUS	β-glucuronidase
GWAS	Genome Wide Association Study
HR	Hypersensitive Response
HRP	Horseradish Peroxidase
IAA	Indole-3-Acetic-Acid
IEF	Isoelectric Focusing
LB	Lysogeny Broth
LPO	Lactoperoxidase
LiP	Lignin Peroxidase
MAMP	Microbe Associated Molecular Pattern
MLO	Myeloperoxidase
MnP	Manganese Peroxidase
PAMP	Pathogen Associated Molecular Pattern
PCATS	Peroxidase-Catalase Superfamily
PCOXS	Peroxidase-Cyclooxygenase Superfamily
PCR	Polymerase Chain Reaction
pI	Isoelectric Point
PI	Propidium Iodide
PNP	Peanut Peroxidase
PRR	Pattern Recognition Receptor
PTI	PAMP Triggered Immunity
qRT-PCR	Quantitative Real-Time PCR
ROS	Reactive Oxygen Species
SBP	Soybean Peroxidase
SDS	Sodium Dodecyl Sulfate
SDS-PAGE	SDS-Polyacrylamide Gel Electrophoresis
SNP	Single Nucleotide Polymorphism
SP	Signal Peptide
SRP	Signal Recognition Particle
TBE	Tris-Borate-EDTA
TE	Tris-EDTA
TPO	Thyroid Peroxidase
VP	Versatile Peroxidase

1. Introduction

Plant pathogens occupy diverse strategies to invade plants and impair their growth and development. In turn, plants have evolved a number of strategies to overcome pathogen infection. However, unlike animals, plants lack an adaptive immune system (Király et al. 2013) and employ mainly two interconnected immune systems to recognize and subsequently respond to pathogen infection (Han, 2018). The first immune system utilizes pattern recognition receptors (PRRs) located at the plant cell surface to recognize microbe associated molecular patterns (MAMPs) present in microbes as well as host-derived damage associated molecular patterns (DAMPs) (Han 2018; Boller & Felix 2009). The other immune system depends on resistance (R) proteins that are produced in response to effector proteins secreted by pathogens to suppress plant immunity (Han 2018). Both of these defense mechanisms require *de novo* protein synthesis and are regulated through complex interconnected signaling pathways.

Among the proteins synthesized, class III plant peroxidases (EC 1.11.1.7; Prxs) are well-known to be produced during infections. They are encoded by large multigene families and are involved in a broad range of physiological processes in plants throughout their life cycle, including cell wall metabolism, defense against pathogen or insect attack, catabolism of auxin, generation of reactive reactive oxygen species (ROS) for oxidative burst or hypersensitive response (HR), and many other processes (Almagro et al. 2009). A previous study by Elfstrand et al. (2020) showed that the gene model MA_10g0010, which encodes a previously uncharacterized class III peroxidase PabPrx86, contains a single nucleotide polymorphism (SNP) that associates with the presence of the pathogen *Thekopsora areolata* in Norway spruce. Therefore, it can be hypothesized that this gene plays a role in the resistance of the tree against this pathogen at the site where infection takes place, possibly through cell wall modification (Elfstrand et al. 2001, Kärkönen et al. 2009, Fagerstedt et al. 2010).

T. areolata is an Eurasian rust fungus with distribution from Europe and northern Asia (Smith et al. 1988) to Russia and Siberia (Kuprevich and Transchel 1957). It causes the cherry spruce rust disease, which is one of the most important macrocyclic cone rusts in Norway spruce, resulting in significant economic losses especially in commercial seed orchards (Kaitera et al. 2014). For instance, 50% to almost 100% of the cones of Norway spruce can be damaged by this pathogen in Norway (Roll-Hansen 1967). Another study by Saho and Takahashi (1970) in Japan reported that the infection of this pathogen resulted in up to 100% empty Japanese spruce seeds, thus threatening the species. Subsequently, Annila and Heliövaara (1991) revealed that *T. areolata* infested up to 15% of Norway spruce cones in a seed orchard in southern Finland. The pathogen was also responsible for the most

of cone rust damages in 2000 (Savonen, 2001) and 2006 (Kaitera et al. 2009). *T. areolata* infects pistillate cones and occasionally shoots of Norway spruce using basidiospores that develop in overwintering *Prunus* leaves (Roll-Hansen 1947). *T. areolata* needs to alter its host between conifers and *Prunus* species to complete its life cycle by producing spores through five distinct stages (Roll-Hansen 1965).

Association of the gene model MA_10g0010 with one of the most important cone rust diseases in Norway spruce is a new finding that has not yet been studied. In the experiments described here, the relative expression level of PaPrx86 in different tissues and different time points of the year were determined in Norway spruce. The peroxidase was expressed and produced in tobacco and its sub-cellular localization was determined.

2. Literature Review

2.1. Norway spruce

Norway spruce (*Picea abies* (L.) Karst.) is one of the most dominant tree species in the boreal forest. It is a member of the Pinaceae family with close genetic distance to *P. asperata*, *P. crassifolia*, and *P. koraiensis* (Ran et al. 2006). It is one of the most widespread tree species in Europe (Meloni et al. 2007), and its natural distribution range in Europe itself can be divided into 3 major regions, namely: Nordic-Baltic-Russian, Hercynian-Carpathian, and Alpine (Skrøppa 2003). As a valuable timber source, Norway spruce has become one of the most commercially and ecologically important conifer species in Europe (Meloni et al. 2007; Skrøppa 2003).

Norway spruce has a long juvenile phase of approximately 20 years before forming the first cones, similar to most conifers. In the late summer of the first-year seedlings, shoot extension stops and terminal buds are formed as a response to the shortening photoperiod. Subsequently, needle primordia are initiated within the buds and frost tolerance starts to develop. During autumn, rest dormancy occurs in the meristem, which will then turn to quiescence dormancy as the temperature decreases up to midwinter, where the frost tolerance is maximal. Lastly, bud burst will occur in the spring when the threshold value of temperature sum has been reached. Growth termination and terminal bud formation in older seedlings and trees occur early in the summer. Regardless, build-up of frost tolerance during late summer is initiated mostly under photoperiodic control (Gyllenstrand et al. 2007). The number of growing days in Norway spruce seedlings are known to be controlled genetically as a response to the photoperiod (Eriksson et al. 1978). Seedlings growing at the northern latitudes have less growing days compared to those from more southern locations.

After reaching maturity, Norway spruce starts to regenerate through sexual reproduction. Spruces are wind-pollinated gymnosperms with both male and female cones on the same plant. Male and female cones (strobili) develop in the early spring, which is then followed by pollination and fertilization. The seeds, which are formed after successful fertilization, will develop after the winter and then mature during the next autumn. Strobilus initiation, optimum pollination, successful fertilization, as well as seed maturation are strongly affected by climatic conditions, requiring moderate to high temperatures and dry conditions during growth season for 2 consecutive years. In the northern latitudes, seed production is often low as a result of rare occurrence of suitable climatic conditions. Thus, in Scandinavia, good seed years are expected only every 10 to 13 years (Andersson 1965; Hagner 1965; Sarvas 1968).

Norway spruce is known to be susceptible to several diseases, including germination failure, damping-off, grey mold, root dieback, snow blights, Scleroderris canker, and Sirococcus blight and

cankers (Lilja et al. 2010). *Thekopsora areolata* (Fr.) Magn., which had been previously discovered to be associated with the peroxidase investigated in this study, causes cone rust in Norway spruce. This pathogen causes significant losses in seed production and germination in Norway spruce orchards (Kaitera & Tillman-Sutela 2014).

2.2. Defense response

As a response to pathogen infections, plants in general – including Norway spruce – employ several strategies to overcome infections. The first barriers that protects plants from pathogen invasion are the cuticle and the cell wall (Bigeard et al. 2015). Cuticle is mainly composed of cutin and waxes (Yeats & Rose 2013), whereas plant cell wall consists of cellulose, hemicellulose, pectin, proteins, and in some cases, lignin, which surrounds the plant cell (Somerville et al. 2004). Together the combination of cuticle and cell wall makes the plant epidermis impenetrable to most pathogens (Bigeard et al. 2015). Nevertheless, natural openings such as lenticels and stomata, as well as wounds resulting from both biotic and abiotic factors can serve as routes for pathogen infection (Melotto et al. 2008; Bigeard et al. 2015). Beside these physical barriers, plants also constitutively produce antimicrobial compounds, which inhibit pathogen growth (Osbourn 1996).

Successful pathogens that can penetrate and survive these barriers then have to withstand the plant immune system, which mainly consists of sophisticated pathogen recognition and defense. This immune system consists of two interconnected branches. The first branch, pathogen associated molecular pattern (PAMP) triggered immunity (PTI), is activated upon the recognition of conserved pathogen or microbial associated molecular patterns (PAMPs or MAMPs) by trans-membrane pattern recognition receptors (PRRs) (Jones & Dangl 2006). In addition, degraded host molecules, known as damage associated molecular patterns (DAMPs), can also induce PTI (Yamaguchi et al. 2010). As a response, plants modulate gene expression as well as signaling pathways to restrict the mobility of pathogen in the host, including stomatal closure (Melotto et al. 2008; Sawinski et al. 2013), generation of ROS (O'Brien et al. 2012), and programmed cell death or hypersensitive response at the site of infection (Mur et al. 2008).

In turn, pathogens can overcome PTI by producing species, race, or even strain specific effector proteins (Avr proteins), which results in effector-triggered susceptibility (ETS). In the second phase of defense, plants co-evolved specific cytoplasmic resistance proteins (R proteins) to recognize the pathogen effector proteins. This induces the effector-triggered immunity (ETI) and subsequently results in hypersensitive response and cross-talk between several defense responses to differentiate biotrophic and necrotrophic pathogens (Jones & Dangl 2006). Nevertheless, plant defense is a

complex system that requires tight regulation of gene expression and signaling pathways. One of the protein groups that are well-known to be induced during plant defense is peroxidases.

2.3. Peroxidases

Peroxidases are enzymes that catalyze reduction of hydrogen peroxide, following the oxidation of a wide range of phenolic and non-phenolic substrate compounds (Pandey et al. 2017). Peroxidases can be found in both prokaryotic and eukaryotic cells in many different organisms, and play an important role in many biological processes, including biodegradation, lignin biosynthesis, and defense mechanisms (Passardi et al. 2005).

2.3.1. Classification

Almost all of the currently known heme peroxidases are divided into two super-families. The first superfamily, known as peroxidase-cyclooxygenase superfamily (PCOXS), is found in animals and plays there a role in defense responses. This superfamily consists of myeloperoxidase (MLO), eosinophil peroxidase (EPO), lactoperoxidase (LPO), and thyroid peroxidase (TPO). The second superfamily, known as the peroxidase-catalase superfamily (PCATS), can be found in bacteria, fungi, and plants (the "non-animal" peroxidase superfamily). It was initially named as bacterial, fungal, and plant heme peroxidase superfamily, but when the Cnidarian peroxidase was discovered, the name of this family changed (González-Rábade et al. 2012; Pandey et al. 2017). This superfamily is further classified into 3 classes, as follows (Pandey 2017):

(a) **Class I peroxidases** are found in both prokaryotic and eukaryotic cells and function mainly in oxidative stress. This includes cytochrome *c* peroxidases (CCP; EC 1.11.1.5), catalase peroxidases (CP; EC 1.11.1.6) and ascorbate peroxidases (APX; EC 1.11.1.11). Cytochrome *c* peroxidases utilize reducing equivalents from cytochrome *c* to reduce hydrogen peroxide into water, whereas ascorbate peroxidases break down hydrogen peroxide using ascorbate as the reducing equivalent. Lastly, catalase peroxidases, which are mainly found in bacteria, have bi-functional activity of both catalase and peroxidase.

(b) **Class II peroxidases** are found only in fungi and they function mainly in lignin biodegradation. This class of peroxidase includes lignin peroxidases (LiP; EC 1.11.1.14), manganese peroxidases (MnP; EC 1.11.1.13) and versatile peroxidases (VP; EC 1.11.1.16). Both LiP and MnP depolymerize lignin and are secreted by lignin-degrading white-rot fungi, of which LiP degrades several phenolic and non-phenolic compounds, whereas MnP catalyzes peroxidase-dependent oxidation of Mn (II) to Mn (III) in the form of oxalate-Mn (III) complex as a redox mediator to oxidize lignin. VPs share a

hybrid structure between LiP and MnP, thus they not only oxidize Mn (II), but also phenolic and non-phenolic compounds similar to LiP in the absence of Mn.

(c) **Class III peroxidases** are widely distributed among plants and are involved in a wide range of physiological processes. This class of peroxidases includes horseradish peroxidases (HRP), soybean peroxidases (SBP), peanut peroxidases (PNP) and many others.

2.3.2. Class III peroxidases

Class III plant peroxidases (EC 1.11.1.7) are one of the best known proteins in plants. They are encoded by large multigene families in all land plants (Duroux and Welinder 2003; Passardi et al. 2004a). Several abbreviations are used to describe class III plant peroxidases, including POD, PER, POX, Prx, and Px, but the best common choice used is Prx (Almagro et al. 2009). Their presence has been reported widely in the plant kingdom, including Chlorophyta, Euglenophyta, Rhodophyta, Byophyta, Pteridophyta, and Spermatophyta (Passardi et al. 2007). In general, this class of peroxidases catalyze reduction of H_2O_2 by taking electrons from donor molecules including lignin precursors, auxin or different secondary metabolites (Hiraga et al. 2001; Passardi et al. 2004b). Together with their large number of isoforms and versality of their catalyzed reactions, they are involved in many physiological processes in plants (Passardi et al. 2005; Almagro et al. 2009; Pandey et al. 2017), such as:

1. Reinforcement of cell walls

   As a response to wounding and pathogen interaction, the cell wall can be rigidified by peroxidases to enhance the physical barrier that limits pathogen invasion, by catalyzing the cross-linking of cell wall components. This includes extension and ferulic acid cross-linking, lignification and suberization.

2. Metabolism of reactive oxygen species (ROS)

   Oxidative burst is one of the most common plant defense responses in the presence of pathogen and their elicitors. Peroxidases may also generate H_2O_2, which can act as a signal to induce programmed cell death (Desikan et al. 2000; Almagro et al. 2009).

3. Production of anti-microbial compounds

   Production of several bioactive plant products have been observed to be synthesized from class III peroxidase mediated reactions (Langcake and Pryce 1977a,b; Langcake 1981; Waffo-Teguo et al. 2001), and the list of both anti-fungal and anti-bacterial compounds as well as other secondary metabolites resulting from class III peroxidase reactions continuously grows.

4. Auxin catabolism

   Class III plant peroxidases also play an essential role in auxin catabolism, either through H_2O_2-dependent pathway or H_2O_2-independent and O_2-dependent pathway (Normanly 1997). Several studies have reported the involvement of peroxidases in auxin related processes. For instance, Gazaryan et al. (1996) and Jansen et al. (2001) observed that over-expression of peroxidases in transgenic tobacco plants showed depressed indole-3-acetic-acid (IAA) levels.

5. Other developmental and stress responses

   In addition to the functions described above, many researches have observed the activity of class III plant peroxidase in many additional plant responses, such as increased peroxidase activity after seed germination (Dendsay & Sachar 1982), increased (Haard 1973; Gorin & Heidema 1976) and decreased (Estrada et al. 2000; Pandey et al. 2012) peroxidase activity during fruit ripening, and changes of expression levels during abiotic stress (Edreva et al. 1998).

3. Objectives

The aims of this study are to:

1. Isolate full length cDNA encoding PabPrx86 from Norway spruce
2. Clone the cDNA in the vector pEAQ-HT-DEST1 for production of the protein in *N. benthamiana*
3. Clone the cDNA with a C-terminal green fluorescence protein (GFP) fusion in the vector pK7FWG2 for protein localization in *N. benthamiana*
4. Analyze the relative expression level of *PabPrx86* in different Norway spruce tissues

4. Materials and Methods

4.1. Sample collection

Terminal buds from a healthy Norway spruce tree (Figure 1) near the Viikki campus of University of Helsinki, Finland (60.219452° N, 25.009002° E), were collected in a clean plastic bag. The number of terminal buds were then counted and weighed to determine the average weight of the buds. In addition, needles, buds, shoots, and lateral buds from Ålbrunna seed orchard, Sweden (59.507597° N, 17.538397° E), were collected with four replicates from different trees at 3 time points (May, June, and September 2019). All samples were kept at -80 ºC until RNA extraction.

Figure 1. The Norway spruce tree in Viikki used for sampling.

4.2. RNA extraction and isolation of full length cDNA for *PabPrx86*

In order to isolate the full length cDNA for *PabPrx86*, RNA from the terminal bud samples collected from Viikki campus were extracted using the pine tree method (Chang et al. 1993). Approximately 100 mg of terminal buds in a 2 ml Eppendorf tube with two metal beads were frozen in liquid nitrogen and ground to powder using mixer mill (Retsch MM 400). 2% of β-mercaptoethanol was added to the RNA extraction buffer (2% PVP, 100 mM Tris-HCl pH 8.0, 25 mM EDTA, 2.0 M NaCl, 0.5 g/L spermidine) and the mixture was heated to 65 ºC. 700 µl of the buffer was added to the powdered ground samples and incubated at 65 ºC for 10 minutes. The RNA was then extracted twice with 600 µl chloroform and centrifuged at 13,300 rpm for 10 minutes. RNA in the upper phase was precipitated by adding 0.25× volumes of 10 M LiCl and left on ice overnight. Precipitated RNA was harvested by

centrifugation at 13,300 rpm for 20 minutes at +4 ºC and washed with 600 µl of cold 70% ethanol. The RNA was allowed to dry for 10 minutes and re-suspended in 50 µl Milli-Q water. Extracted RNA was checked for its quality and quantity using gel electrophoresis and NanoDrop Lite spectrophotometer (Thermo Scientific), respectively, and stored at -80 ºC.

Extracted RNA was reverse transcribed to cDNA using Super Script III Reverse Transcriptase (Invitrogen by Thermo Fisher Scientific) according to the manufacturer's instructions using oligo-dT as primer. The *PabPrx86* encoding sequence was isolated and amplified using Polymerase Chain Reaction (PCR) with the following primer pair (designed based on the gene sequence from Congenie website (http://congenie.org/gene?id=MA_10g0010#sequence), with a part of the Gateway attB attachment site for recombination):
GER1624 5'–AAAAAGCAGGCTCCATGGGGGCTGCAGCTTTGTA–3' and
GER1625 5'–AGAAAGCTGGGTCTAGTTGTAGTTGTTGAAGG–3'. The following reagents were put into PCR tube: 17.4 µl Milli-Q water, 5 µl 5× Phusion buffer, 0.5 µl 10 mM dNTP mix, 0.125 µl Phusion enzyme, 0.5 µl primer GER1624F (10 pmol/µl), 0.5 µl primer GER1625R (10 pmol/µl), and 1 µl cDNA template. The PCR reaction was then run using the following program: initial denaturation 95 ºC for 3 minutes, followed by 30 cycles consisting of denaturation 94 ºC for 1 minute, annealing 55 ºC for 30 seconds, elongation 72 ºC for 2 minutes, and post-PCR 15 ºC. Subsequently, 5 µl of the PCR product was further amplified in PCR using the following primer pair that generates the complete attB site:
GER29F 5'–GGGGACAAGTTTGTACAAAAAAGCAGGCT–3' and
GER30R 5'–GGGGACCACTTTGTACAAGAAAGCTGGGT–3'; 95 ºC for 1 minute, for 5 cycles: 94 ºC for 30 seconds, 45 ºC for 30 seconds, 72 ºC for 1 minute, and following 10 cycles: 94 ºC for 30 seconds, 55 ºC for 30 seconds, 72 ºC for 1 minute, after that post-PCR 15 ºC. The products from these PCR reactions were visualized on 0.8% agarose gel in 0.5× Tris-Borate-EDTA (TBE) buffer (44.5 mM Tris, 44.5 mM boric acid, 1 mM EDTA) using ethidium bromide (EtBr) and purified using Roche purification kit.

In addition, another PCR reaction was run separately using primer pair designed at 60 bp upstream and downstream from the *PabPrx86* gene:
GER1622F 5'–AAGAGCCAGCACTACTAGGC–3' and
GER1623R 5'–GCAGTCCACACTTGGAGCAA–3'. The product from this PCR was sent to Macrogen Europe B.V., Amsterdam for sequencing to determine the full length sequence of *PabPrx86*. Full length *PabPrx86* was confirmed by comparing the sequencing result with database from Congenie (http://congenie.org/gene?id=MA_10g0010#sequence).

4.3. Gateway cloning of *PabPrx86* and transformation to *Escherichia coli* DH5α

After the full length sequence of *PabPrx86* was confirmed, the second PCR product from the two-step PCR was cloned to the entry vector pDONR221 (Invitrogen by Thermo Fisher Scientific, Figure 2) by BP reaction using the following reagents: PabPrx86 fragment from second PCR (150 ng), pDONR221 (150 ng) in 8 µl 10 mM Tris-HCl, 1 mM EDTA, pH 8 Tris-EDTA (TE) buffer, and 2 µl BP clonase II enzyme mix (Invitrogen by Thermo Fisher Scientific). The mixture was incubated overnight at room temperature. After that, 1 µl Proteinase K (Invitrogen by Thermo Fisher Scientific) was added, and the mixture was incubated at 37 ºC for 10 minutes. 5 µl of the cloning mixture was transformed to *E. coli* competent cells in 1.5 ml Eppendorf tube, first thawing the competent cells in the tube on ice for 20 minutes. The mixture was chilled on ice for 30 minutes and then heat-shocked at 42 ºC for 30 seconds. After that, 1 ml of Lysogeny Broth (LB) was added and the tube was incubated at 37 ºC for 1 hour. After centrifugation at 2500 ×g for 3 minutes, most of the supernatant was removed, leaving ca. 200 µl. The cells were re-suspended in the remaining supernatant and spread on LB agar with 50 µg/ml kanamycin and grown at 37 ºC for overnight. Four colonies were pure cultured and their plasmid were isolated using GenElute Plasmid Miniprep Kit (Sigma-Aldrich) and analyzed by digestion with *Pst*I and *Bam*HI. Plasmids showing correct band pattern were then sent for sequencing to further confirm their insert, and the strains carrying plasmids that showed correct sequence were stored in glycerol at -80 ºC.

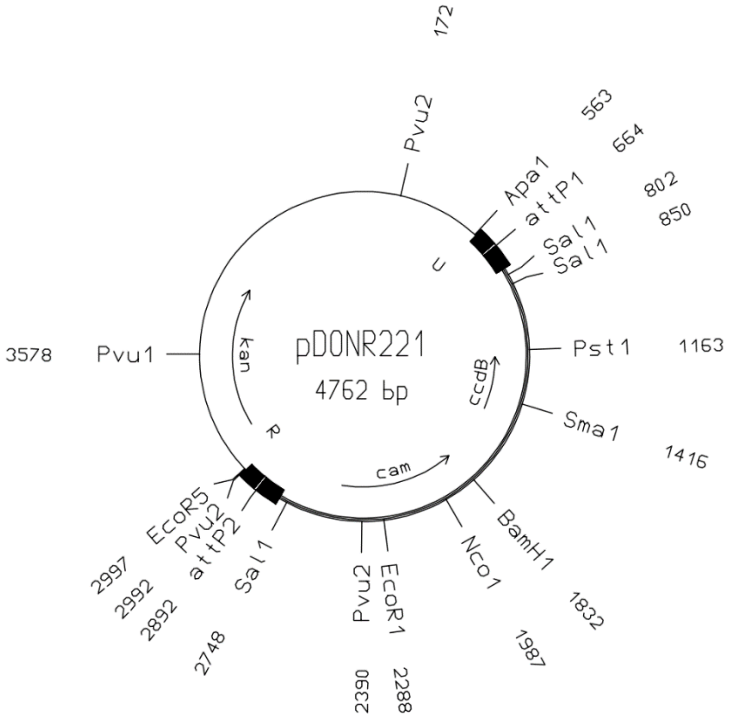

Figure 2. Structure of the plasmid pDONR221.

4.4. Transformation to *Agrobacterium* and expression in tobacco

Plasmid pDONR221 with *PabPrx86* insert from the previous step was cloned to the hypertranslatable expression plasmid pEAQ-HT-DEST1 (Sainsbury et al. 2009), which also includes the expression of 35S-P19 silencing suppressor (Figure 3). The cloning was done using a similar protocol as for the BP reaction but with LR clonase II enzyme mix (Invitrogen by Thermo Fisher Scientific). After that, plasmid pEAQ-HT-DEST1 with insert sequence was transformed to *E. coli* DH5α. Colonies carrying the correct construct were selected using the boiling prep method (Harwood, 1996) followed by restriction enzyme digestion, and plasmids from promising colonies were isolated using GenElute Plasmid Miniprep Kit and checked by restriction enzyme digestion. Confirmed plasmids were then transformed to *A. tumefaciens* strain C58C1(pGV2260) (Deblaere et al. 1985) with rifampicin, carbenicillin, and kanamycin selection (100 µg/ml each) and incubated for 2-3 days at 28 ºC. Subsequently, the transformed and pure cultured *A. tumefaciens* were inoculated in 5 ml LB medium, grown overnight shaking at 28 ºC, pelleted and adjusted to OD_{600} = 0.5 in 10 mM $MgCl_2$, 10 mM MES-KOH pH 6.0, 200 µM acetosyringone buffer. The mixture was injected to leaves of six-week old *N. benthamiana* plants using the agro-infiltration method (Li 2011). After infiltration, the plants were grown for 3 days and the leaves were harvested and analyzed.

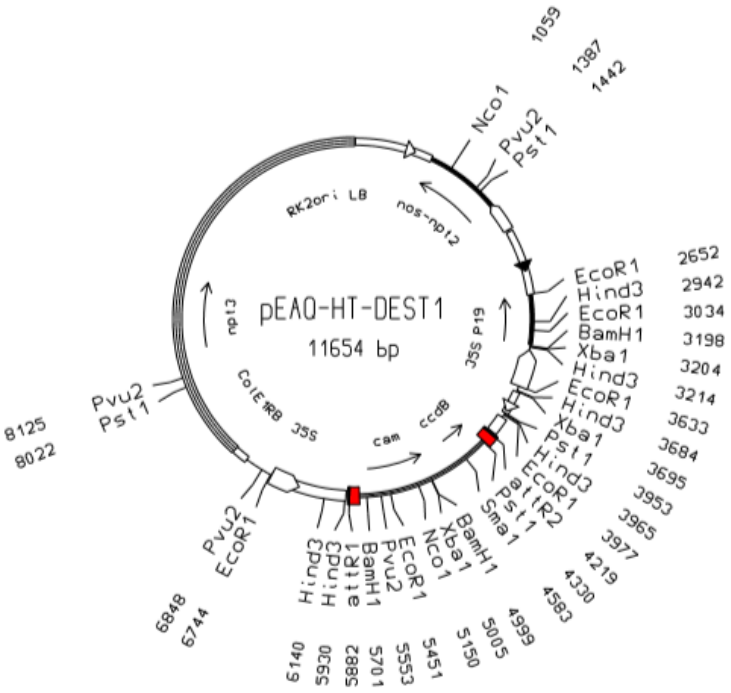

Figure 3. Structure of the plasmid pEAQ-HT-DEST1.

4.5. Enzymatic assays

4.5.1. Protein extraction

200 mg of the harvested leaves from agro-infiltrated tobacco was frozen in liquid nitrogen and milled to powder with steel beads using the mixer mill Retsch MM 400 for 2×30 seconds at 30 Hz. Milled tissues were then stored at -80 ºC until further use. In order to extract the total protein from the leaves, 800 µl of cold extraction buffer (100 mM Tris-HCl pH 7.5, 1 tablet/10 ml Roche EDTA-free protease inhibitor, 2 µl/ml β-mercaptoethanol) was added and then incubated on ice for 10 – 15 minutes. Cell debris was centrifuged at maximum speed for 10 minutes at 4 ºC. The supernatant was transferred to a clean 1.5 ml Eppendorf tube and centrifuged again. The supernatant from second centrifugation was then collected in a new tube, and total protein content was measured in enzyme-linked immunosorbent assay (ELISA) plate according to the method described by Bradford (1976), by measuring the optical density at 595 nm using bovine serum albumin (BSA) as standard. Glycerol was added to 20% and the extracted protein was stored in -80 ºC until further use.

4.5.2. Activity staining and SDS-polyacrylamide gel electrophoresis (SDS-PAGE)

Activity staining of peroxidase was performed on precast any kD polyacrylamide gel (Bio-Rad Mini-PROTEAN TGX Gels) with and without 0.1% sodium dodecyl sulfate (SDS) in reservoir buffer (25 mM Tris, 192 mM glycine, pH 8.8) using the Mini Protean III Electrophoresis Cell (Bio-Rad). After that, peroxidases were detected by soaking the gel in 15 mM phosphate buffer pH 6.0 containing 1 mM guaiacol and 1 mM H_2O_2. Color development was observed in 10 minutes. Subsequently, the gel was transferred to Coomasive blue staining solution for 24 hours and then destained in water for 48 hours. Molecular weight of the PabPrx86 protein was calculated using Bioinformatics Resource Portal exPASy (https://web.expasy.org/compute_pi/).

4.5.3. Isoelectric focusing

Isoelectric focusing (IEF) was performed in 4% polyacrylamide gel (11 cm × 22 cm) containing pharmalyte with pH range from 3.5 to 10.0 using the Multiphor II (Pharmacia) apparatus. Extracted protein samples were pipetted into the well strip and focused using constant power at 10 W for 2 hours. After the run, peroxidases were visualized by transferring and staining the gel in 50 mM Na-acetate buffer pH 5.0 containing 10 mM $CaCl_2$ and 0.08% (w/v) 3,3'-diaminobenzidine (DAB). After adding 1/100 volume of 50 mM H_2O_2 into the solution, peroxidase activity appeared as brown bands in the gel. The pH gradient of the gel was determined by cutting strips from the middle part of the gel every 0.5 cm in a region where the samples were not pipetted in. The strips were then equilibrated in 1 ml of Milli-Q water overnight at 4 ºC, and the pH gradient was determined by

measuring the pH of the liquid phase and plotted as standard curve. Predicted isoelectric point (pI) of PabPrx86 was estimated using Bioinformatics Resource Portal exPASy (https://web.expasy.org/compute_pi/), whereas the observed experimental pI was determined by regression line of the standard curve using the position of the band in the gel.

4.6. Localization of PabPrx86

4.6.1. PCR reaction and Gateway cloning

Protein from PabPrx86 was visualized by fusing the expressed protein with green fluorescence protein (GFP). 100 ng of the plasmid from the construct described above was amplified with two-step PCR with primer pair

GER1624F 5'–AAAAAGCAGGCTCCATGGGGGCTGCAGCTTTGTA–3' and

GER1626R2 5'–AGAAAGCTGGGTCGTTGTAGTTGTTGAAGG–3' for the first PCR reaction and GER29F and GER30R for the second PCR reaction. GER1626R2 does not include the stop codon of *PabPrx86*, allowing its fusion to GFP. The product was cloned to pDONR221 using gateway BP reaction, transformed to *E. coli* DH5α, and subsequently the plasmid was extracted and sequenced similarly as described above. Colonies containing the plasmid with correct sequence were stored in glycerol at -80 ºC.

4.6.2. Transformation to *Agrobacterium* and visualization of PabPrx86 protein

In order to visualize the localization of the PabPrx86 protein, the entry vector pDONR221 inserted with *PabPrx86* gene without stop codon from the previous step was cloned to pK7FWG2 (Figure 4) using LR reaction. The procedure of *E. coli* transformation, verification, *Agrobacterium* transformation and agro-infiltration of *N. benthamiana* leaves was done as in 4.3 and 4.4, except that spectinomycin was used instead of kanamycin for selection of the expression plasmid. The plants were grown for 3 days, and the infiltrated leaves were cut and observed under epifluorescence microscope (Axio Imager M2) to determine the location of the protein in the cells.

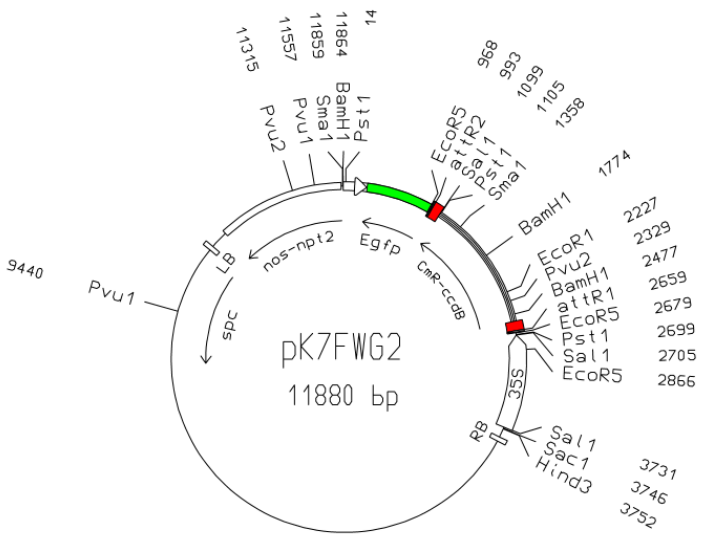

Figure 4. Structure of the plasmid pK7FWG2.

4.7. Relative expression level of *PabPrx86* in different Norway spruce tissues

Relative expression level of *PabPrx86* was determined by extracting the total RNA from several Norway spruce tissues (needles, stem, bud, and lateral bud) using the RNA extraction method as described in 4.2. The extracted RNA was digested with DNase and purified in a NucleoSpin® RNA Clean-up XS Binding Column (Macherey-Nagel). The quantity and quality of the purified RNA was observed by measuring the concentration using NanoDrop Lite spectrophotometer (Thermo Scientific) and running 500 ng of the RNA in 0.8% agarose gel electrophoresis in 0.5× TBE. Subsequently, the RNA samples were reverse transcribed to cDNA using 500 ng of the RNA template as described in 4.1 above. Synthesized cDNA samples were diluted 5×, and used for quantitative real-time PCR (qRT-PCR) with the following reagents: 7.5 µl LightCycler 480 SYBR Green I Master (Roche Diagnostics GmbH), 1.5 µl forward primer (5 pmol/µl), 1.5 µl reverse primer (5 pmol/µl), and 4.5 µl diluted cDNA. The primer pair used for PabPrx86 was

GER1658 (5'–TACTCTTTCTGGCGGTCACA–3') and

GER1659 (5'– CCTTTCATGGCGTTGTGATA 3'). As references to determine relative expression levels of *PabPrx86* also transcripts for the constitutively expressed genes for phosphoglucomutase

GER1674 (5'–AATGCAGTTGAAGCCATTCC–3') and

GER1675 (5'–CCAGTGCCGAAACTCTCTTC–3') (Vestman et al. 2010), and elongation factor 1α

GER1676 (5'–TAGTCCCTCACAGCAAAACGA–3') and

GER1677 (5'–TTAAGAATGGAGATGCCGGGTTTGT–3') (Arnerup et al. 2011) were amplified. All primer pairs lead to amplification of a fragment of a size in the range of 115-247 bp. Relative expression level was calculated using the ΔΔCt method (Livak & Schmittgen 2001). The efficiency of amplification for each primer pair was determined by running one of the samples in a 10× serial

dilution from 1 to10^{-5}, and efficiency was calculated from the slope value of each primer pair using the regression $E = 10^{(-1/slope)}$.

5. Results

5.1. Cloning and sequencing of full length *PabPrx86* cDNA

As the first step to study the expression of *PabPrx86* in Norway spruce, the full length *PabPrx86* cDNA was obtained by extracting total RNA from bud samples collected from a spruce individual growing in Viikki, Helsinki (Figure 1). The coding sequence of this gene was amplified using PCR. A band of 990 bp in agarose gel indicated that the gene was indeed expressed in the bud samples.

Sequencing of the fragment showed that there were two allelic variants of the gene, with 8 nucleotides differences and without frameshifts. These allelic variants were observed as double signals in the sequencing chromatogram (Figure 5, indicated by arrows). The fragment was cloned into pDONR221 vector and three resulting plasmids were sequenced. This showed that the nucleotides corresponding to the lower signals always coincided in one of the plasmids, and those to the higher signals in the two other plasmids. This result suggested that the difference in peak size at the variant positions was due to different amount of steady-state mRNA of two alleles in the sample, allele with lower signal level had a lower expression level in the mRNA population than the other allele. The less expressed allele was named as the minor allele (annotated as plasmids pST4-2 and pST5-2, *Agrobacteriums* STAT4-2 and STAT5-2, and the protein as PabPrx86-2), and the other one as the major allele (annotated as plasmids pST4-4 and pST5-4, *Agrobacteriums* STAT4-4 and STAT5-4, and the protein PabPrx86-4). Interestingly, the *PabPrx86* sequence from Congenie database showed at these positions either the minor or the major allele nucleotide, except for one single base at position 297 (Figure 6). This suggests that the Swedish spruce populations sequenced for Congenie (Nystedt et al. 2013) harbor the same two alleles isolated in this study, and further that there is more allelic variation present in the nature, but not very much more.

Using the translated nucleotide sequences, the presence of a signal peptide was predicted using SignalP-5.0 (http://www.cbs.dtu.dk/services/SignalP/). Signal peptide was predicted at the N-terminus of both PabPrx86-2 and PabPrx86-4, with the predicted cleavage site appearing between amino acids A and Q at positions 23 and 24 (Figure 6). The predicted molecular weight and pI of PabPrx86 protein was estimated from the amino acid sequences excluding the signal peptide using Bioinformatics Resource Portal exPASy (https://web.expasy.org/compute_pi/), with predicted molecular weight of 33.43 and 33.47 kD and predicted pI of 6.58 and 7.09 for PabPrx86-2 and PabPrx86-4, respectively.

Both allelic forms were cloned in the destination vector pEAQ-HT-DEST1 (pST4-2 for minor allele and pST4-4 for major allele; Figure 7A) and pK7FWG2 with C-terminus GFP tag (pST5-2 and pST5-4; Figure 7B), and subsequently transformed to *A. tumefaciens* C58C1(pGV2260) (Table 1) and agro-infiltrated to *N. benthamiana*.

Table 1. List of *Agrobacterium* strains and the plasmids they harbor.

Agrobacterium strain	Plasmids
STAT4-2	pGV2260 and pST4-2
STAT4-4	pGV2260 and pST4-4
STAT5-2	pGV2260 and pST5-2
STAT5-4	pGV2260 and pST5-4

5.2. Protein yields

Leaf samples at the infiltration spot were used as material for protein extraction. In addition to the *PabPrx86* constructs, total soluble protein from leaves with uninfiltrated and infiltrated with *Agrobacterium* carrying the 35S-P19 alone, as negative controls, were also extracted to observe if the infiltration treatment itself caused any changes in their protein content, particularly in peroxidases. Total amount of crude protein (Table 2) was determined after extraction by comparing the absorbance at 595 nm (A_{595}) with Bovine Serum Albumin (BSA) standard (A_{595} = 1.00 corresponds to 8 µg BSA in the 2 µl sample).

Table 2. Concentration of crude protein extracted from inoculated *N. benthamiana* leaves.

Sample	Absorbance (A_{595})	Total protein content (µg)	Concentration (µg/µl)
Control	0.496	3.97	1.99
P19	0.368	2.94	1.47
STAT4-2a	0.604	4.83	2.42
STAT4-2b	0.736	5.89	2.95
STAT4-4a	0.532	4.26	2.13
STAT4-4b	0.493	3.94	1.97

The yield of total protein from uninfiltrated leaf samples and leaves infiltrated with *A. tumefaciens* carrying P19 were 3.97 and 2.94 µg, respectively, whereas the average yield of total protein from leaves infiltrated with *A. tumefaciens* carrying pST4-2 and pST4-4 were 5.36 and 4.10 µg, respectively (Table 2). Subsequently, the presence of the peroxidase was then observed using the SDS-PAGE method.

Figure 5. Sequencing chromatogram of the *PabPrx86* cDNA PCR fragment from the Norway spruce tree in Viikki, Helsinki. Arrows on the peaks indicate the positions where the two of allelic variants differ. One of the allelic variants shows systematically a lower signal.

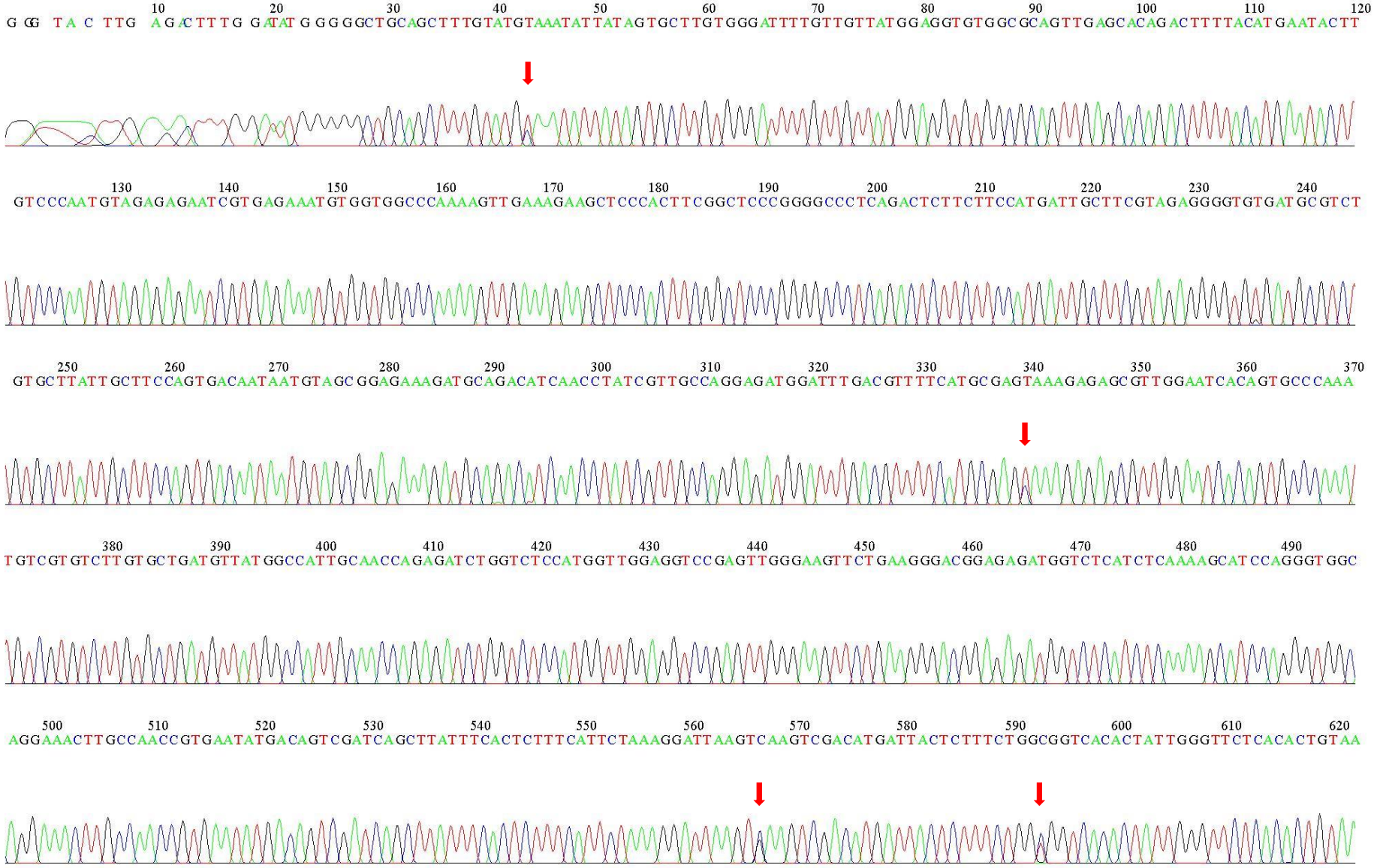

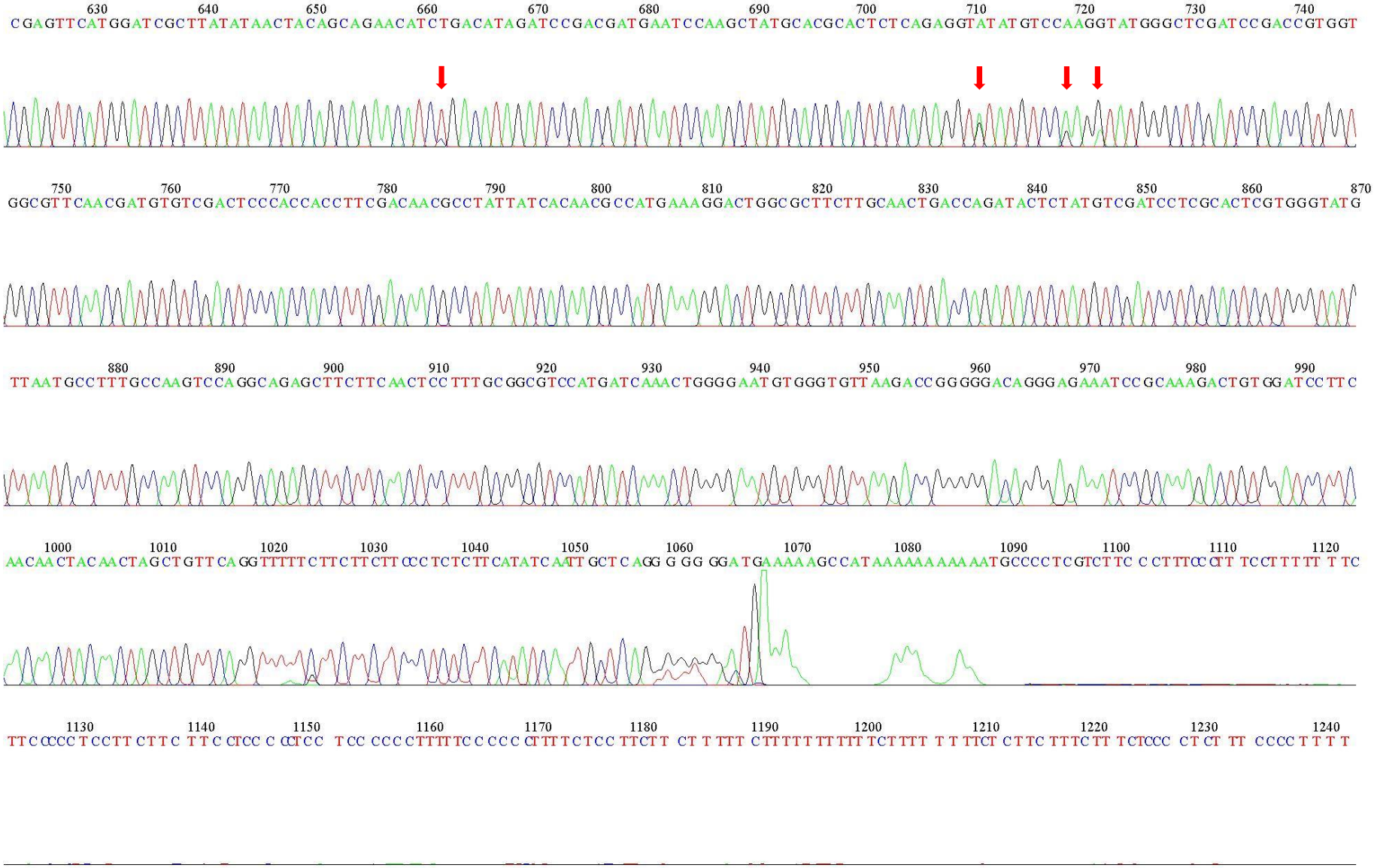
630 640 650 660 670 680 690 700 710 720 730 740
CGAGTTCATGGATCGCTTATATAACTACAGCAGAACATCTGACATAGATCCGACGATGAATCCAAGCTATGCACGCACTCTCAGAGGTATATGTCCAAGGTATGGGCTCGATCCGACCGTGGT
750 760 770 780 790 800 810 820 830 840 850 860 870
GGCGTTCAACGATGTGTCGACTCCCACCACCTTCGACAACGCCTATTATCACAACGCCATGAAAGGACTGGCGCTTCTTGCAACTGACCAGATACTCTATGTCGATCCTCGCACTCGTGGGTATG
880 890 900 910 920 930 940 950 960 970 980 990
TTAATGCCTTTGCCAAGTCCAGGCAGAGCTTCTTCAACTCCTTTGCGGCGTCCATGATCAAACTGGGGAATGTGGGTGTTAAGACCGGGGGACAGGGAGAAATCCGCAAAGACTGTGGATCCTTC
1000 1010 1020 1030 1040 1050 1060 1070 1080 1090 1100 1110 1120
AACAACTACAACTAGCTGTTCAGGTTTTTCTTCTTCTTCCCTCTCTTCATATCAATTGCTCAGGGGGGATGAAAAAGCCATAAAAAAAAAAAATGCCCCTCGTCTTCCCTTTCCCTTTCCTTTTTTCTC
1130 1140 1150 1160 1170 1180 1190 1200 1210 1220 1230 1240
TTCCCCCTCCTTCTTCTTCCTCCCCCTCCTCCCCCCTTTTTCCCCCCTTTCTCCTTCTTCTTTTTTTTTTTTCTTTTTTTTCTTCTTTCTTCTCTCCCCTCTCTTCCCCTTTTT

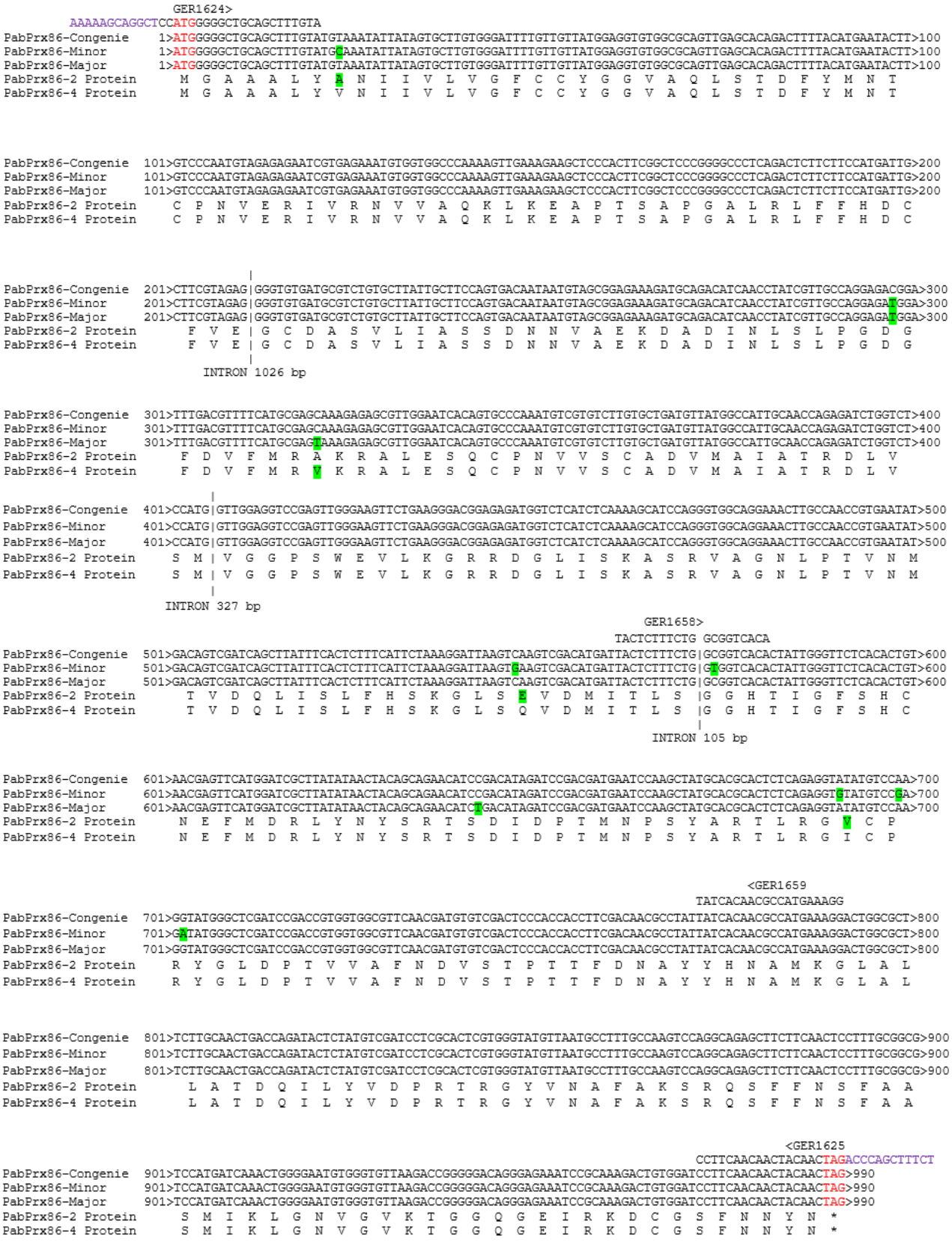

Figure 6. Multiple comparisons between the nucleotide sequences of *PabPrx86* from Congenie database and the two allelic variants isolated in this study, and amino acid sequences between PabPrx86-2 and PabPrx86-4. Position of primers used for cloning and for qPCR are shown on the sequence.

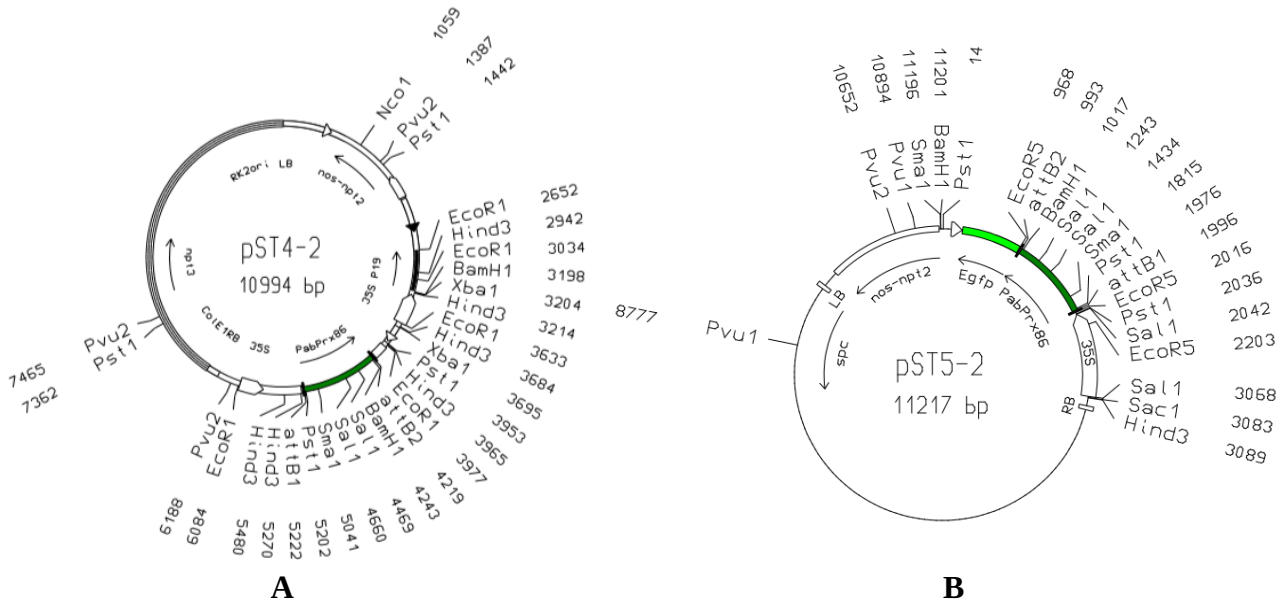

Figure 7. Structure of (A) pST4-2; and (B) pST5-2 with PabPrx86 insert driven by 35S promoter.

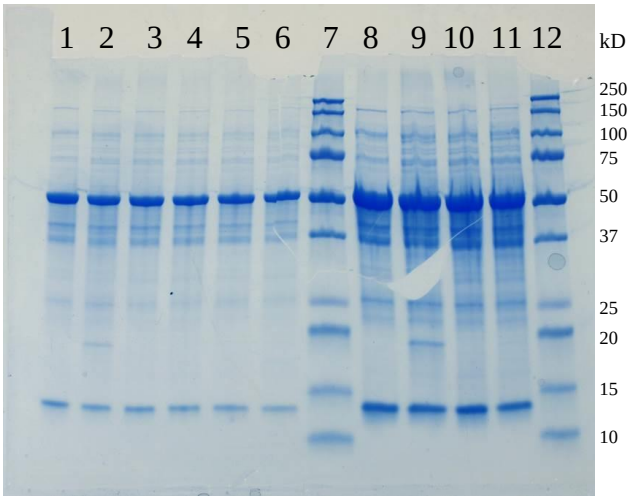

Figure 8. Soluble protein extracts (6 and 18 µg loaded in the gel for lane 1-6 and lane 8-11, respectively) from *N. benthamiana* leaves agro-infiltrated with constructs carrying: (1) & (8): negative control; (2) & (9): P19 silencing suppressor; (3) & (10): pST4-2 (PabPrx86-2)-a; (4): pST4-2 (PabPrx86-2)-b; (5) & (11): pST4-4 (PabPrx86-4)-a; (6): pST4-4 (PabPrx86-4)-b; and (7) & (12): Precision Plus Protein™ Dual Colors Standard (BioRad). No additional band of PabPrx86 was detected at the predicted size of 33 kD.

In SDS-PAGE, no additional band of expected size (ca. 33 kD) could be observed in the soluble protein extracts from infiltrated samples (Figure 8). However, the native gel (Figure 9A and B) showed peroxidase activity. Although faint bands could be observed also in the negative control and P19 treatments, clearer bands indicating stronger peroxidase activity appeared for both PabPrx86-2 and PabPrx86-4.

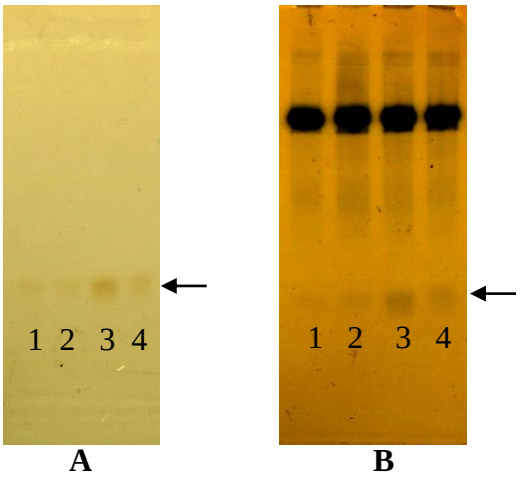

Figure 9. (A) Activity staining of PabPrx86 using guaiacol and H_2O_2 (pointed by arrow); (B) PabPrx86 after double staining with Coomassie blue (pointed by arrow): (1) negative control; (2) P19 silencing suppressor; (3) PabPrx86-2; (4) PabPrx86-4. Bands indicate the presence of peroxidase activity.

When the peroxidase isoforms were separated using IEF, different patterns were observed for the minor and major allele (Figure 10). One strong band could be observed for both PabPrx86-2 and PabPrx86-4. Using the linear regression of the standard curve (Figure 11), the pI of both bands showed the value of 8.21 for PabPrx86-2 and 8.35 for PabPrx86-4. Very faint peroxidase bands were also detected from the soluble protein extract of negative control and P19 infiltrated samples, both at similar pI of 8.18.

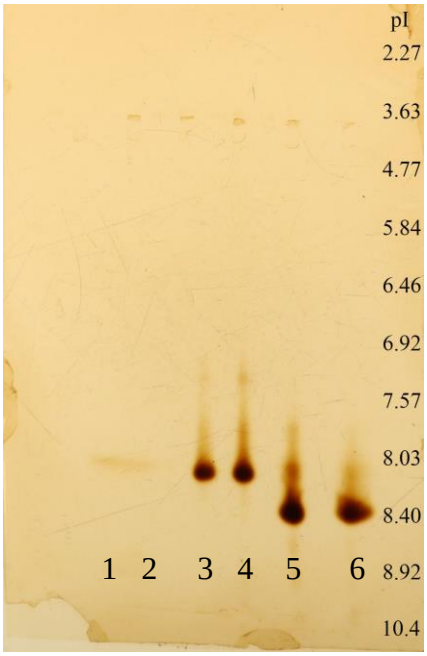

Figure 10. Isoelectric focusing on PabPrx86 peroxidase produced from (1) negative control; (2) P19 silencing suppressor; (3) pST4-2A; (4) pST4-2B; (5) pST4-4A; and (6) pST4-4B.

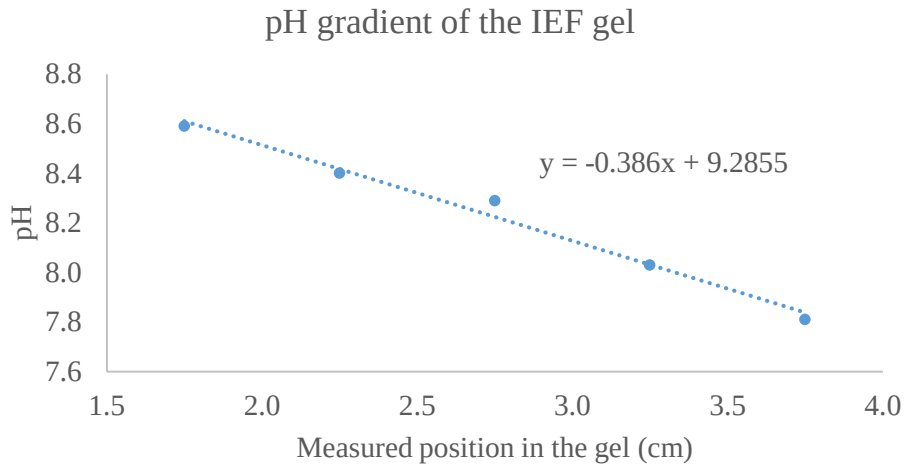

Figure 11. pH gradient of the IEF gel. Isoelectric point of PabPrx86 was calculated from the band position on the gel using the regression line of the curve.

5.3. Sub-cellular localization of the protein from PabPrx86

In order to investigate the sub-cellular localization of the PabPrx86 protein, C-terminal GFP fusions of PabPrx86 was transiently expressed in *N. benthamiana*, and their localization was observed with epifluorescence microscope. *Agrobacterium* expressing P19 protein (Figure 12A, GFP) was used as negative control and showed no GFP signal (only weak auto-fluorescence), whereas the presence of PabPrx86 protein tagged with GFP fusion (35S-PabPrx86-2-GFP and 35S-PabPrx86-4-GFP; Figure 12B and 12C GFP, respectively) led to a bright green signal under the microscope. 35S-mGFP4 (Figure 12D) and 35S-mGFP5-ER (Figure 12E) were used as positive controls, leading to a cytoplasmic and secreted GFP, respectively. By comparing the merged DAPI-GFP channel of PabPrx86 with mGFP4 and mGFP5-ER, it can be seen that PabPrx86 protein for both major and minor allele looked very similar to the one of mGFP5-ER, of which the GFP signal was not detected on the nucleus of the cell, indicating that the protein was translated at endoplasmic reticulum (ER) ribosomes.

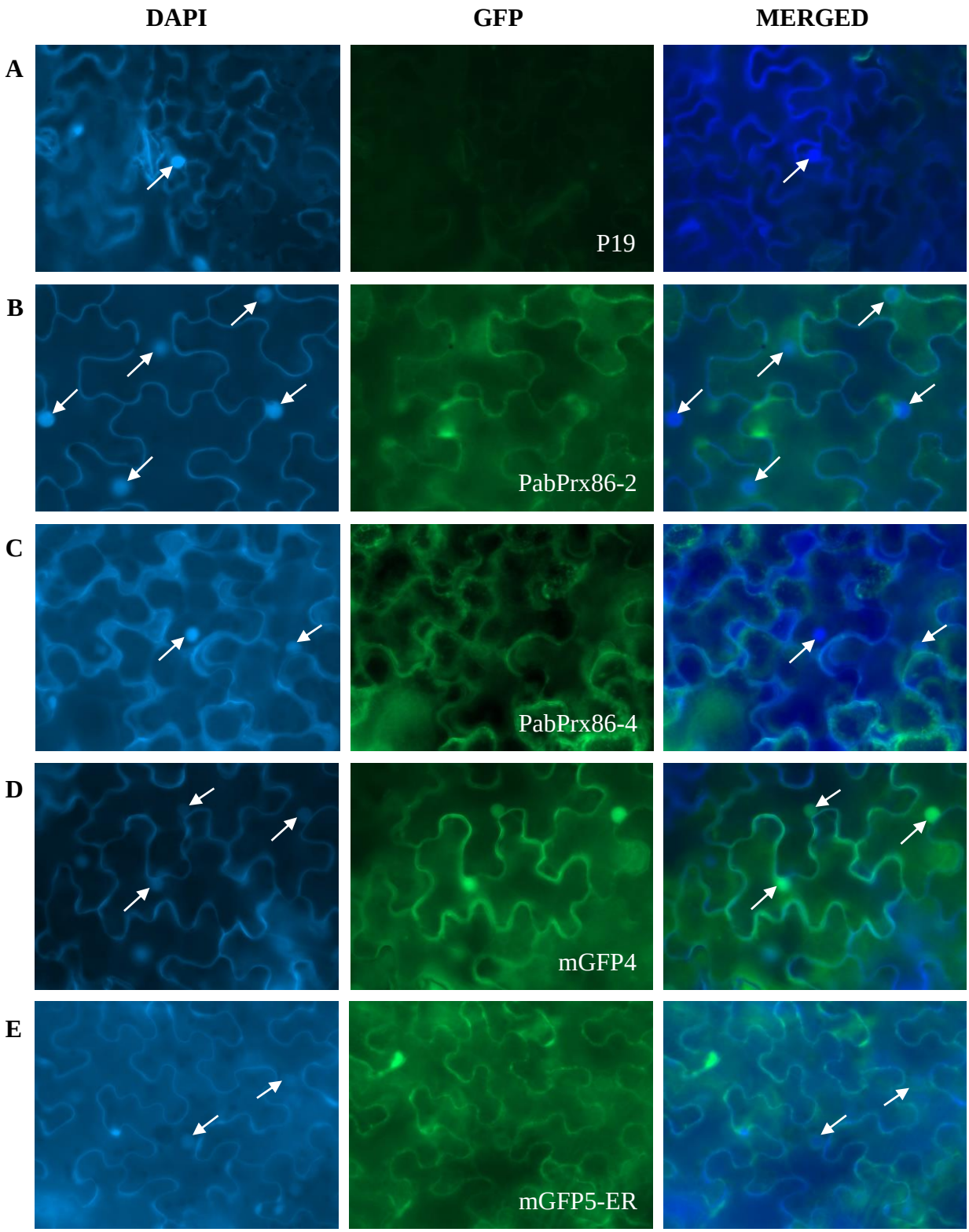

Figure 12. Epifluorescence micrograph of *N. benthamiana* infiltrated with *A. tumefaciens* carrying (A) 35S-P19 silencing suppressor showing no GFP but auto-fluorescence; (B) 35S-PabPrx86-2-GFP (PabPrx86 minor allele); (C) 35S-PabPrx86-4-GFP (PabPrx86 major allele); (D) 35S-mGFP4; and (E) 35S-mGFP5-ER. The cytoplasmic mGFP4 stains the nucleus, but the secreted mGFP5-ER and the PabPrx86-GFP fusions, do not. Arrows indicate the position of nuclei.

5.4. Relative expression level of *PabPrx86*

To quantify the relative expression level of *PabPrx86* gene in different spruce tissues and different times of the year, a gene specific primer pair was designed. The forward primer was designed on the last intron boundary of the *PabPrx86* coding sequence from Congenie database to avoid false positive signals from genomic DNA amplification. Amplification efficiency for *PabPrx86*, elongation factor-1α and phosphoglucomutase were calculated as 2.04, 2.04, and 2.01, respectively. These values indicated that the polymerase enzyme worked at full capacity and two copies of the sequences were generated during each cycle of the PCR. The expression level of *PabPrx86* was different between different tissues on different time of the year (Figure 13). The highest expression level in the needle and stem was detected on May, which were significantly down-regulated in June and September. Later in the season, the expression was associated with buds and lateral buds, with the highest expression level was observed in June.

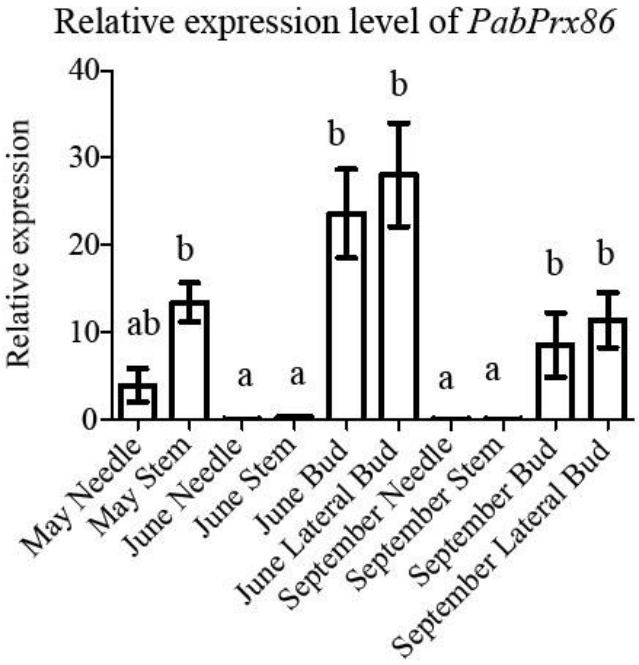

Figure 13. Relative expression level of *PabPrx86* in different tissues across different time points of the year.

6. Discussion

MA_10g0010 is a gene model in the Norway spruce genome that was predicted to encode a previously undescribed peroxidase (PabPrx86). Previous study by Elfstrand et al. (2020) showed in a genome wide association study (GWAS) that a single nucleotide polymorphism (SNP), discovered through exome capture and Illumina sequencing, in the first intron of *PabPrx86* gene is associated with the presence of the pathogen *Thekopsora areolata*. In order to gain further understanding about its expression in Norway spruce, this gene was analyzed from spruce samples from Viikki in Helsinki, Finland and Ålbrunna seed orchard, Sweden by carrying out an assay for the protein expressed from the gene, observing its sub-cellular localization, as well as comparing its relative expression level amongst different tissues at different times of the year.

Two allelic variants of *PabPrx86* were discovered, first in the form of double signals in the sequencing chromatogram and subsequently by isolating the corresponding cDNA molecules. Both variants encode a protein with 329 amino acids, similar to the prediction from Congenie database (http://congenie.org/gene?id=MA_10g0010#sequence). Interestingly, the nucleotide sequence in the Congenie database shows a mixture of the major and minor alleles at the variant positions observed in this study, except for a single base difference at position 297, indicating that some further polymorphism of *PabPrx86* is present in the locus in addition to the two Viikki variants found in this study. It is not known if the *T. areolata* associated SNP positioned in an intron of *PabPrx86*, is associated with one of the allelic variants found in Viikki. Based on the amino acid sequences, the molecular weight of PabPrx86 protein was predicted to be 33.43 and 33.47 kD for the two allelic variants of PaPrx86. These values are well in the range of molecular weights for class III plant peroxidases, which is between 28 and 60 kD (Hiraga et al. 2001).

Leaves infiltrated with *A. tumefaciens* carrying the constructed plasmids expressed the PabPrx86 protein driven by the 35S promoter in the constructs (Figure 7). Odell et al. (1985) reported that 35S promoter is a strong constitutive promoter with no tissue specificity of expression. In SDS-PAGE, no additional bands at the predicted molecular weight could be observed between the soluble protein extracts from infiltrated samples as compared to controls. This result indicates that if PabPrx86 is expressed in tobacco, it is below the level of detection by the Coomassie Brilliant Blue G-250 stain (20-40 ng of protein, which would equal to approximately 0.3% of the 6 µg total soluble protein loaded in the gel). This amount is fairly high for transient expression through agro-infiltration. For example, Andrews & Curtis (2008) measured transient β-glucuronidase (GUS) expression in different tobacco leaves and found that the highest expression level achieved by leaf infiltration in *N. benthamiana* was 0.025% of total soluble protein. Guaiacol staining of the native gel revealed weak

peroxidase bands from both samples producing PabPrx86-2 and PabPrx86-4, suggesting that the peroxidases produced were indeed present but in small amounts. This result is similar to the one of Shimoni and Reuveni (1988), where several peroxidase bands were revealed after double staining with guaiacol and subsequently Coomasie blue. In addition to PabPrx86-2 and PabPrx86-4, both uninfiltrated and P19 controls also showed faint peroxidase bands, which may be a native peroxidase produced by the tobacco. Nevertheless, the stronger peroxidase activity as compared to controls observed from this result showed that the infiltrated constructs showed promising expression in *N. benthamiana*.

Isoelectric focusing, on the other hand, showed prominent bands for PaPrx86. Both expressed peroxidases had basic observed pIs, which were 8.21 and 8.35 for PabPrx86-2 and PabPrx86-4, respectively. These values are considerably higher compared to the predicted pI from ExPASy, which are 6.58 and 7.09. Several previous studies have shown that post-translational modifications can result in significantly different pI than predicted. For instance, Koutaniemi et al. (2015) suggested that the differences between calculated and observed pI on laccase could be due to glycosylation. Similarly, Kumar et al. (2004) observed that there was a direct correlation between the number of phosphorylation conferred and the change of pI of the respective protein, and that proteins with lower molecular weight and basic initial pI showed greatest shift in pI upon phosphorylation. Furthermore, Shaw et al. (2001) also explained that the estimated pI often disagrees with observed pI as the pK_a values used for the calculation are usually obtained from model compounds, which may differ significantly with the pK_a of groups in folded proteins. Similar to the result observed in the native gel, faint peroxidase bands were also observed in the uninfiltrated and P19 controls in the IEF gel with slightly lower pI, suggesting that they are different peroxidase isoforms produced by the tobacco itself. In any case, peroxidase isoforms are present in a wide range of pI, from acidic to basic (Hoyle, 1977; Gabaldón et al. 2005), and although estimated isoelectric point is an important parameter, several factors like post-translational modifications, biochemical alterations, and the pK_a values used in the calculation itself may affect the estimated value. Moreover, the strong peroxidase bands observed on PabPrx86-2 and PabPrx-4 in the IEF gel directly showed that the *PabPrx86* gene indeed codes for a peroxidase.

Prediction based on amino acid sequence of PabPrx86 indicates that the protein has a signal peptide (SP) in its N-terminus. Signal peptides are short N-terminal amino acid sequences of newly synthesized proteins that target the respective protein into or across membranes (Armenteros et al. 2019). The presence of SPs is recognized by signal recognition particle (SRP), which will then deliver the ribosome to ER membrane (Walter & Johnson 1994). After translation is concluded, the protein can either stay in the ER as resident protein or proceed to the Golgi complex to be delivered to its

target site in the endomembrane system (Geva & Schuldiner, 2014). Using this principle as a baseline, two references were selected in this experiment: 35S-mGFP4, which shows expression in the cytosol and nucleus due to the absence of a SP (Grebenok et al. 1997; Köhler 1998; Kwok & Hanson 2004), and 35S-mGFP5-ER, which contains not only signaling peptide to be targeted to the ER, but also ER-retention motif HDEL at the C-terminal end to retain it in the ER (Gomord et al. 1997, Di Sansebastiano 1998). Although epifluorescence micrographs of PabPrx86-GFP fusion were not able to pinpoint exactly the subcellular localization of the fusion protein, the 35S-PabPrx86-GFP construct avoided the nucleus, similar to the 35S-mGFP5-ER construct used as one of the references in this experiment. In contrast, 35S-mGFP4 showed GFP signal on the nucleus. Together with the presence of signal peptides at the N-terminus of the protein, this result indicated that both proteins were translated at ER-bound ribosomes. Despite not being able to precisely detect the subcellular localization of PabPrx86 protein, many previous studies have demonstrated class III peroxidases as apoplastic protein that plays important roles in plants. For instance, Polle et al. (1994) discovered that apoplastic peroxidases participate in lignin formation in Norway spruce. Minibayeva et al. (2015) also observed that apoplastic peroxidases interplay with other enzymes to initiate oxidative burst and produce ROS. As class III plant peroxidases play roles in many physiological processes in plants, it is highly likely that PabPrx86 is a secreted apoplastic protein due to its solubility, and its localization correlates strongly with its main function in Norway spruce.

Using qRT-PCR, the relative expression level of *PabPrx86* was shown to peak in buds and lateral buds in June. This result may reveal the role of *PabPrx86* in Norway spruce, as the expression pattern of proteins in plants often has strong correlation with its function. For instance, Kim et al. (2012) demonstrated that genes encoding class III plant peroxidases were more highly expressed in cold tolerant brassinosteroid-insensitive mutant (*bri1-9*) of *Arabidopsis thaliana,* thus suggesting its role in increased cold tolerance. Moural et al. (2017) also observed that the that the expression level of switchgrass peroxidase *PviPRX9* was correlated with its function, where it peaked in June during rhizome development, followed by intermediate expression in July and August when the rhizome growth slows, and subsequently down-regulated in September due to senescence. In addition, there was expression of the *PabPrx86* in the needle and stem in May, which may be related to bud break or flush process as mentioned previously by Elfstrand et al. (2020). Expression of *PabPrx86* therefore strongly depends on the types of tissues and the time of the year, which may be related to specific developmental processes in the buds or flushing shoots or female cones of Norway spruce, as all of these organs have the bud as common basis. This developmental process will then in turn determine whether the successful colonization of the pathogen *T. areolata*. The expression pattern of PabPrx86 observed in this study is in line with the one demonstrated in exAtlas

(http://congenie.org/gene?id=MA_10g0010#expression), which shows that the expression level of *PabPrx86* was higher in August than in September 2010 in the buds, but in the vegetative shoots (stem and needle) was moderate during May 2010 and totally absent in June 2010 (Figure 13A).

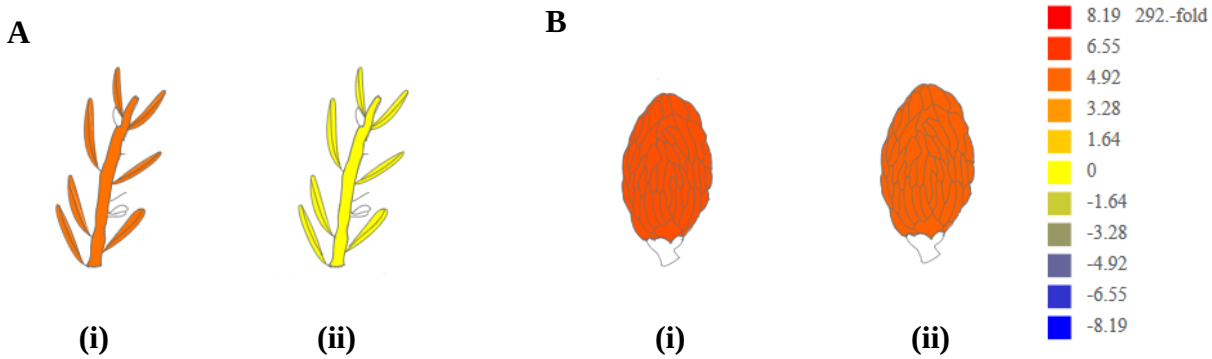

Figure 13. Expression level of PabPrx86 in (A) bud on (i) May 27, 2010, (ii) June 21, 2010; and (B) bud on (i) August 12, 2010, (ii) September 7, 2010. Source: Congenie database.

Class III plant peroxidases have been long studied and shown to play important roles in plants, including activation of defense mechanisms against pathogens and physiological processes such as lignification. *PabPrx86*, which was previously undescribed and predicted to encode for peroxidase in Norway spruce, has been expressed in a plant system. In this study, two *PabPrx86* allele variants from Norway spruce tree in Viikki, Helsinki were isolated. Isoelectric focusing and DAB staining results showed that *PabPrx86* indeed codes for peroxidase with basic pI, whereas subcellular localization and expression analysis showed that this gene was targeted to the ER and had the highest expression in the buds and lateral buds in June. Although the specific role of peroxidase from *PabPrx86* is still unclear, the result of this study has demonstrated a number of important characteristics of *PabPrx86* from Norway spruce. Furthermore, the methods used in this study also provided a general but important characterization of a novel enzyme, which unlocks more interesting research opportunities. Although it is unknown whether if the SNP was the causative reason for the association of *PabPrx86* with *T. areolata*, it is reasonable and interesting to inspect *PabPrx86* as a candidate gene. Linkage disequilibrium is very low in conifers, meaning that associated markers are very close (less than 1 kb away) from the causative mutations (Neale & Savolainen 2004). Future work includes more sequence and bioinformatics analysis on the SNP and how it associates with the allelic forms of *PaPrx86* (the ones observed here, or others). Moreover, in order to understand a more specific role of *PabPrx86* in Norway spruce, disease scoring of *T. areolata* against different variants of *PabPrx86* as well as its expression level after infection and protein-protein interaction and post-translational modifications such as glycosylation should be investigated.

7. Conclusion

Peroxidases are enzymes encoded by large gene families and they catalyze reduction of hydrogen peroxide and concomitant oxidation of many different substrate compounds. They have been long known to participate in many important physiological processes in plants. This study began from the observation that a SNP in the intron of Norway spruce gene model MA_10g0010 has a strong correlation with the presence of pathogen *T. areolata* in vegetative buds. The gene model was predicted to code for a previously uncharacterized peroxidase, PaPrx86. In this study, several characteristics of PabPrx86 were analyzed, including the expression of PabPrx86 in spruce and production of the protein in tobacco.

The first discovery found after the full length of PabPrx86 was successfully isolated and sequenced was that there were two allelic variants in the Norway spruce bud samples from Viikki, Helsinki, with 8 nucleotides difference from each other and expressed at slightly different level. After the gene was cloned and expressed in *N. benthamiana*, analysis of the total soluble protein detected that both the major and minor allele of *PabPrx86* indeed code for peroxidase with slightly different basic pI. Although the epifluorescence microscopy result was not able to pinpoint the exact localization of PabPrx86 in the cell, it can be concluded that PabPrx86 completed its translation at the ER-bound ribosomes due to the fact that signal peptide was presence at the N-terminus of the protein and it showed similar appearance under epifluorescence microscope, as a C-terminal GFP fusion, to the secreted reference mGFP5-ER. Relative expression analysis on several Norway spruce tissue samples from different time points showed that there was moderate expression of the gene in the needle and stem in May, but later in the season the expression was associated with the buds and lateral buds, which may indicate its importance in developmental processes at organs with buds as common basis, and subsequently influence successful pathogen infections. The actual role of *PabPrx86* is still unclear and further experiments are still required, thus providing interesting research opportunities for the future.

Acknowledgements

This study was carried out during September 2019 to February 2020 at the Gerbera laboratory of University of Helsinki in Finland. First of all, I would like to express my deepest gratitude to my main supervisor, Prof. Teemu Teeri, for his excellent advices and guidance both during the laboratory work and construction of this master's thesis. He has taught me a lot about scientific thinking by his vast knowledge and experiences of molecular biology, plant secondary metabolism, and also science in general. In addition, he also holds crayfish party – or *rapujuhlat* – annually, which was the best that I have ever had and I am very much looking forward to attend in the coming years! I would also like to thank my co-supervisors, Prof. Åke Olson and Prof. Malin Elfstrand from the Swedish University of Agricultural Sciences in Uppsala, not only for providing me a very interesting research topic, but also for the samples and guidance during this master's thesis. I am very excited to discuss about what we will do with our peroxidase!

Special thanks to Anna Kärkönen from LUKE and the members of Gerbera laboratory at University of Helsinki – Prof. Paula Elomaa, Anu Rokkanen, Marja Huovila, Eija Takala, Soile Jokipii-Lukkari, Feng Wang, Teng Zhang, Lingping Zhu, Md. Minhazur Rahman, Saku Mattila, and Bishawjet Das – for taking your time to guide me with the laboratory work and also for creating a lovely environment in the laboratory. I also thank my emPLANT friends – Diana Laura Labastida Jaimes, Attiq Ur-Rehman, Temurkhan Ayupov, Madan Kafle, Matthieu Mitchel, Jinghong Lu, Guillaume Bergon, Marissa Barbosa, Selman Yeşilkaya and everyone others – for all the memories that we have gone through during this master's program. Thanks also to my friends and classmates – Peter Halvarsson, Mahdiyyah Ardhina, Emil Bengtsson, Olof Sundström, Daniela Kreber, Shannon Mustard, Danielle Curran, and everyone from PPI Uppsala and others that I cannot mention one by one – for all the assistance, fun, and laughter, and also for listening to my non-sense. I miss and love you all!

Finally, I would also thank Erasmus Mundus scholarship and also all coordinators and administrators in emPLANT program – Alicia Ayerdi-Gotor, Anders Kvarnheden, Guénolé Boulch, Aude Martin, Viola Niklander-Teeri, Minna Haapalainen and others for funding and your assistance that make my master's study possible. And lastly, I would like to express my most sincere thanks to my parents and families for their continuous love and support. Thank you everyone!

8. References

Almagro, L., Ros, L.V.G., Belchi-Navarro, S., Bru, R., Barcelo, A.R. & Pedreno, M.A. 2009. Class III peroxidases in plant defence reactions. *Journal of Experimental Botany* 60: 377-390

Andersson, E. 1965. Cone and seed studies in Norway spruce (*Picea abies* [L.] Karst.). *Studia Forestalia Suecica* 23: 5-214

Andrews, L.B. & Curtis, W.R. 2005. Comparison of transient protein expression in tobacco leaves and plant suspension culture. *Biotechnology Progress* 21: 946-952

Annila, E. & Heliövaara, K. 1991. Chemical control of cone pests in a Norway spruce seed orchard. *Silva Fennica* 25: 59–67

Arnerup, J., Lind, M., Olson, Å., Stenlid, J., & Elfstrand, M. 2011. The pathogenic white-rot fungus *Heterobasidion parviporum* triggers non-specific defence responses in the bark of Norway spruce. *Tree Physiology* 31: 1262-1272

Bigeard, J., Colcombet, J. & Hirt, H. 2015. Signaling mechanisms in Pattern-Triggered Immunity (PTI). *Molecular Plant* 8: 521-539

Boller, T. & Felix, G. 2009. A renaissance of elicitors: perception of microbe-associated molecular patterns and danger signals by pattern-recognition receptors. *Annual Review of Plant Biology* 60: 379–406

Bradford, M.M. 1976. A rapid and sensitive method for the quantitation of microgram quantities of protein utilizing the principle of protein-dye binding. *Analytical Biochemistry* 72: 248-254

Chang, S., Puryear, J. & Cairney, J. 1993. A simple and efficient method for isolating RNA from pine trees. *Plant Molecular Biology Reporter* 11: 113-116

Cheng, Y.W., Qi, Y.C., Zhu, Q., Chen, X., Wang, N., Zhao, X., Chen, H.Y., Cui, X.J., Xu, L.L. & Zhang, W. 2009. New changes in the plasma-membrane-associated proteome of rice roots under salt stress. *Proteomics* 9: 3100-3114

Deblaere, R., Bytebier, B., De Greve, H., Deboeck, F., Schell, J., Van Montagu, M., & Leemans, J. 1985. Efficient octopine Ti plasmid-derived vectors forAgrobacterium-mediated gene transfer to plants. *Nucleic Acids Research* 13: 4777–4788

Dendsay, J.P.S. & Sachar, R.C. 1982. Hormonal control of peroxidase activity and its relationship with growth in mung bean seedlings. *Plant Science Letters* 26: 251-256

Desikan, R., Hancock, J.T., Coffey, M.J. & Neill, S.J. 2000. Hydrogen peroxide induced gene expression in *Arabidopsis thaliana*. *Free Radical Biology and Medicine* 28: 773-778

Di Sansebastiano, D.P., Paris, N., Marc-Martin, S. & Neuhaus, J.M. 1998. Specific accumulation of GFP in a non-acidic vacuolar compartment via a C-terminal propeptide-mediated sorting pathway. *The Plant Journal* 15: 449-457

Duroux, L. & Welinder, K.G. 2003. The peroxidase gene family in plants: A phylogenetic review. *Journal of Molecular Evolution* 57: 397-407

Edreva, A., Yordanov, I., Kardjieva, R. & Gesheva, E. 1998. Heat shock responses of bean plants: involvement of free radicals, antioxidants and free radical/active oxygen scavenging systems. *Biologia Plantarum* 41: 185-191

Elfstrand, M., Fossdal, C., Sitbon, F., Olsson, O., Lönneborg, A. & von Arnold, S. 2001. Overexpression of the endogenous peroxidase-like gene spi 2 in transgenic Norway spruce plants results in increased total peroxidase activity and reduced growth. *Plant Cell Reports* 20: 596-603

Elfstrand, M., Zhou, L.H., Baison, J., Olson, Å., Lunden, K., Karlsson, B., Wu, H.X., Stenlid, J. & Garcia-Gil, M.R.G. 2020. Spruce genetic variation shapes its fungal community. *Molecular Ecology* 29: 199-213

Eriksson, G., Ekberg, I., Dormling, I., Matern, B. & von Wettstein, D. 1978. Inheritance of bud-set and bud-flushing in *Picea abies* (L.) Karst. *Theoretical and Applied Genetics* 52: 3-19

Estrada, B., Bernal, M.A., Diaz, J., Pomar, F. & Merino, F. 2000. Fruit development in *Capsicum annum*: changes in capsaicin, lignin, free phenolics, and peroxidase patterns. *Journal of Agricultural and Food Chemistry* 48: 6234-6239

Fagerstedt, K.V., Kukkola, E.M., Koistinen, V.V.T., Takahashi, J. & Marjamaa, K. 2010. Cell wall lignin is polymerized by class III secretable plant peroxidases in Norway spruce. *Journal of Integrative Plant Biology* 52: 186-194

Gabaldón, C., López-Serrano, M., Pedreño, M.A., & Barceló, A.R. 2005. Cloning and molecular characterization of the basic peroxidase isoenzyme from *Zinnia elegans*, an enzyme involved in lignin biosynthesis. *Plant Physiology* 139: 1138-1154

Gazaryan, I.G., Lagrimini, L.M., Ashby, G.A. & Thorneley, R.N. 1996. Mechanism of indole-3-acetic acid oxidation by plant peroxidases: anaerobic stopped-flow spectrophotometric studies on horseradish and tobacco peroxidases. *Biochemical Journal* 313: 841-847

Geva, Y. & Schuldiner, M. 2014. The back and forth of cargo exit from the endoplasmic reticulum. *Current Biology* 24: R130-R136

Gomord, V., Denmat, L.A., Fitchette-Laine, A.C., Satiat-Jeunemaitre, B., Hawes, C. & Faye, L. 1997. The C-terminal HDEL sequence is sufficient for retention of secretory proteins in the endoplasmic reticulum (ER) but promotes vacuolar targeting of proteins that escape the ER. *The Plant Journal* 11: 313-325

González-Rábade, N., Oliver-Salvador, M.C., Salgado-Manjarrez, E. & Badillo-Corona, J.A. 2012. In vitro production of plant peroxidases – A review. *Applied Biochemistry and Biotechnology* 166: 1644-1660

Gorin, N. & Heidema, F.T. 1976. Peroxidase activity in golden delicious apples as a possible parameter of ripening and senescence. *Journal of Agricultural and Food Chemistry* 24: 200-201

Grebenok, R.J., Pierson, E., Lambert, G.M., Gong, F.C., Afonso, C.L., Haldeman-Cahill, R., Carrington, J.C. & Galbraith, D.W. 1997. Green-fluorescent protein fusions for efficient characterization of nuclear targeting. *The Plant Journal* 11: 573-586

Gyllenstrand, N., Clapham, D., Källman, T. & Lagercrantz, U. 2007. A Norway spruce FLOWERING LOCUS T homolog is implicated in control of growth rhythm in conifers. *Plant Physiology* 144: 248-257

Haard, N.F. 1973. Upsurge of particulate peroxidase in ripening banana fruit. *Phytochemistry* 12: 555-560

Hagner, S. 1965. Cone crop fluctuations in Scots pine and Norway spruce. *Studia Forestalia Suecica* 33: 1-21

Han, G.Z. 2018. Origin and evolution of the plant immune system. *New Phytologist* 222: 70-83

Harwood A.J. 1996. The rapid boiling method for small-scale preparation of plasmid DNA. In: Harwood A.J. (eds) Basic DNA and RNA Protocols. Methods in Molecular Biology™ 58. Humana Press

Hiraga, S., Sasaki, K., Ito, H., Ohashi, Y. & Matsui, H. 2001. A large family of class III peroxidases. *Plant & Cell Physiology* 42: 462-468

Hoyle, M.C. 1977. High resolution of peroxidase-indoleacetic acid oxidase isoenzymes from horseradish by isoelectric focusing. *Plant Physiology* 60: 787-793

Jansen, M.A.K., van den Noort, R.E., Tan, M.Y.A., Prinsen E., Lagrimini, L.M. & Thorneley, R.N.F. Phenol-oxidizing peroxidases contribute to the protection of plants from ultraviolet radiation stress. *Plant Physiology* 126: 1012-1023

Jones, J.D. & Dangl, J.L. 2006. The plant immune system. *Nature* 444: 323-329

Kaitera, J., Hiltunen, R., Kauppila, T., Pitkäranta, M. & Hantula, J. 2014. Fruiting and sporulation of *Thekopsora* and *Chrysomyxa* cone rusts in *Picea* cones and *Prunus* leaves. *Forest Pathology* 44: 387-395

Kaitera, J. & Tillman-Sutela, E. 2014. Germination capacity of *Thekopsora areolata* aeciospores and the effect of cone rusts on seeds of *Picea abies*. *Scandinavian Journal of Forest Research* 29: 22-26

Kärkönen, A., Warinowski, T., Teeri, T.H., Simola, L.K. & Fry, S.C. 2009. On the mechanism of apoplastic H_2O_2 production during lignin formation and elicitation in cultured spruce cells – Peroxidases after elicitation. *Planta* 230: 553-567

Kim, B.H., Kim, S.Y. & Nam, K.H. 2012. Genes encoding plant-specific class III peroxidases are responsible for increased cold tolerance of the *brassinosteroid-insensitive 1* mutant. *Molecules and Cells* 34: 539-548

Király, L., Künstler, A., Bacso, R., Hafez, Y.M. & Király, Z. 2013. Similarities and differences in plant and animal immune systems – what is inhibiting pathogens? *Acta Phytopathologica et Entomologica Hungarica* 48: 187-205

Koutaniemi, S., Malmberg, H.A., Simola, L.K., Teeri, T.H. & Kärkönen, A. 2015. Norway spruce (*Picea abies*) laccases: characterization of a laccase in a lignin-forming tissue culture. *Journal of Integrative Plant Biology* 57: 341-348

Köhler, R.H. 1998. GFP for *in vivo* imaging of subcellular structures in plant cells. *Trends in Plant Science* 3: P317-P320

Kumar, Y., Khachane, A., Belwal, M., Das, S., Somsundaram, K. & Tatu, U. 2004. ProteoMod: A new tool to quantitate protein post-translational modifications. *Proteomics* 4: 1672-1683

Kuprevich, V. & Transchel, V. 1957. Cryptogamic plants of the USSR. Volume 4. Moscow, Russia: USSR Academy of Sciences

Kwok, E.Y. & Hanson, M.R. 2004. Plastids and stromules interact with the nucleus and cell membrane in vascular plants. *Plant Cell Reports* 23: 188-195

Langcake, P. 1981. Disease resistance of *Vitis* spp. and the production of the stress metabolites resveratrol, e-viniferin, a-viniferin and pterostilbene. *Physiological Plant Pathology* 18: 213-226

Langcake, P. & Pryce, R.J. 1977a. A new class of phytoalexins from grapevines. *Experientia* 33: 151-152

Langcake, P. & Pryce, R.J. 1977b. The production of resveratrol and the viniferins by grapevines in response to ultraviolet irradiations. *Phytochemistry* 16: 1193-1196

Li, X. 2011. Agroinfiltration of *Nicotiana benthamiana* protocol for transient expression via Agrobacterium. *Bio-101*: e95

Lilja, A., Poteri, M., Petäistö, R.L., Rikala, R., Kurkela, T. & Kasanen, R. 2010. Fungal diseases in forest nurseries in Finland. *Silva Fennica* 44: 525-545

Livak, K.J. & Schmittgen, T.D. 2001. Analysis of relative gene expression data using real-time quantitative PCR and the 2(-delta delta C(T)) method. *Methods* 25: 402-408

Meisrimler, C.N., Planchon, S., Renaut, J., Sergeant, K. & Lüthje, S. 2011. Alteration of plasma membrane-bound redox systems of iron deficient pea roots by chitosan. *Journal of Proteomics* 74: 1437-1449

Meloni, M., Perini, D. & Binelli, G. 2007. The distribution of genetic variation in Norway spruce (*Picea abies* Karst.) populations in the western Alps. *Journal of Biogeography* 34: 929-938

Melotto, M., Underwood, W. & He, S.Y. 2008. Role of stomata in plant innate immunity and foliar bacterial diseases. *Annual Review of Phytopathology* 46: 367-386

Minibayeva, F., Beckett, R.P. & Kranner, I. Roles of apoplastic peroxidases in plant response to wounding. *Phytochemistry* 112: 122-129

Moural, T.W., Lewis, K.M., Barnaba, C., Zhu, F., Palmer, N.A., Sarath, G., Scully, E.D., Jones, J.P., Sattler, S.E. & Kang, C.H. 2017. Characterization of class III peroxidases from switchgrass. *Plant Physiology* 173: 417-433

Mur, L.A., Kenton, P., Lloyd, A.J., Ougham, H. & Prats, E. 2008. The hypersensitive response: the centenary is upon us but how much do we know? *Journal of Experimental Botany* 59: 501-520

Neale, D.B. & Savolainen, O. 2004. Association genetics of complex traits in conifers. *Trends in Plant Science* 9: 325-330

Normanly, J. 1997. Auxin metabolism. *Physiologia Plantarum* 100: 431-442

Nystedt, B., Street, N.R., Wetterbom, A. *et al*. 2013. The Norway spruce genome sequence and conifer genome evolution. *Nature* 497: 579-584

Odell, J.T., Nagy, F. & Chua, N.H. 1985. Identification of DNA sequences required for activity of the cauliflower mosaic virus 35S promoter. *Nature* 313: 810-812

Osbourn, A.E. 1996. Preformed antimicrobial compounds and plant defense against fungal attack. *Plant Cell* 8: 1821-1831

O'Brien, J.A., Daudi, A., Butt, V.S. & Bolwell, G.P. 2012. Reactive oxygen species and their role in plant defence and cell wall metabolism. *Planta* 236: 765-779

Pandey, V.P., Awasthi, M., Singh, S., Tiwari, S., & Dwivedi, U.N. 2017. A comprehensive review on function and application of plant peroxidases. *Biochemistry & Analytical Biochemistry* 6: 1-16

Pandey, V.P., Singh, S., Singh, R. & Dwivedi, U.N. 2012. Purification and characterization of peroxidase from papaya (*Carica papaya*) fruit. *Applied Biochemistry and Biotechnology* 167: 367-376

Passardi, F., Cosio, C., Penel, C. & Dunand, C. 2005. Peroxidases have more functions than a Swiss army knife. *Plant Cell Reports* 24: 255-265

Passardi, F., Longet, D., Penel, C. & Dunand, C. 2004a. The class III peroxidase multigenic family in rice and its evolution in land plants. *Phytochemistry* 65: 1879-1893

Passardi, F., Penel, C. & Dunand, C. 2004b. Performing the paradoxical: how plant peroxidases modify the cell wall. *Trends in Plant Science* 9: 534-540

Passardi, F., Zamocky, M., Favet, J., Jakopitsch C., Penel, C., Obinger, C. & Dunand C. 2007. Phylogenetic distribution of catalase-peroxidases: are these patches of order in chaos? *Gene* 397: 101-113

Polle, A., Otter, T. & Seifert, F. 1994. Apoplastic peroxidases and lignification in needles of Norway spruce (*Picea abies* L.). *Plant Physiology* 106: 53-60

Ran, J.H., Wei, X.X. & Wang, X.Q. 2006. Molecular phylogeny and biogeography of *Picea* (Pinaceae): Implications for phylogeographical studies using cytoplasmic haplotypes. *Molecular Phylogenetics and Evolution* 41(2): *405–419*

Roll-Hansen, F. 1947. New information of the spruce cone rust (*Pucciniastrum padi*). *Meddelelser fra det Norske Skogsforsoksvesen* 9: 503-510

Roll-Hansen, F. 1965. *Pucciniastrum areolatum* on *Picea engelmannii*: Identification by spermogonia. *Meddelelser fra det Norske Skogsforsoksvesen* 20: 389-397

Roll-Hansen, F. 1967. On diseases and pathogens on forest trees in Norway 1960-1965. *Meddelelser fra det Norske Skogsforsoksvesen* 21: 173-262

Saho, H., Takahashi, I. 1970. Inoculation experiments of *Thekopsora areolata* (Fr.) Magnus, a cone rust of *Picea* spp. in Japan. *Transactions of the Mycological Society of Japan* 11: 109-112

Sainsbury, F., Thuenemann, E.C. & Lomonossoff, G.P. 2009. pEAQ: versatile expression vectors for easy and quick transient expression of heterologous proteins in plants. *Plant Biotechnology Journal* 7: 682-693

Sarvas, R. 1968. Investigations on the flowering and seed crop of *Picea abies*. *Communicationes Instituti Forestalis Fenniae* 67: 1-84

Savonen, E.M. 2001. Spruce had a good cone year but suffered a large amount of damage. *Taimiuutiset* 1: 10-13

Sawinski, K., Mersmann, S., Robatzek, S. & Bohmer, M. 2013. Guarding the green: pathways to stomatal immunity. *Molecular Plant Microbe Interaction* 26: 626-632

Shaw, K.L., Grimsley, G.R., Yakovley, G.I., Makarov, A.A. & Pace, C.N. 2001. The effect of net charge on the solubility, activity, and stability of ribonuclease Sa. *Protein Science* 10: 1206-1215

Shimoni, M. & Reuveni, R. 1988. A method for staining and stabilizing peroxidase activity in polyacrylamide gel electrophoresis. *Analytical Biochemistry* 175: 35-38

Skrøppa, T. 2003. EUFORGEN Technical Guidelines for genetic conservation and use for Norway spruce (*Picea abies*). International Plant Genetic Resources Institute, Rome, Italy. 6 pages

Somerville, C., Bauer, S., Brininstool, G., Facette, M., Hamann, T., Milne, J., Osborne, E., Paredez, A., Persson, S., Raab, T., Vorwerk, S. & Youngs H. 2004. Toward a systems approach to understanding plant cell walls. *Science* 306: 2206-2211

Vestman, D., Larsson, E., Uddenberg, D., Cairney, J., Clapham, D., Sundberg, E. & von Arnold, S. 2010. Important processes during differentiation and early development of somatic embryos of Norway spruce as revealed by changes in global gene expression. *Tree Genetics and Genomes* 7: 347-362

Waffo-Teguo, P., Lee, D., Cuendet, M., Merillon, J.M., Pezzuto, J.M. & Kinghorn, A.D. 2001. Two new stillbene dimer glucosides from grape (*Vitis vinifera*) cell cultures. *Journal of Natural Products* 64: 136-138

Walter, P. & Johnson, A.E. 1994. Signaling sequence recognition and protein targeting to the endoplasmic reticulum membrane. *Annual Review of Cell Biology* 10: 87-119

Yamaguchi, Y., Huffaker, A., Bryan, A.C., Tax, F.E. & Ryan, C.A. 2010. PEPR2 is a second receptor for the Pep1 and Pep2 peptides and contributes to defense responses in *Arabidopsis*. *The Plant Cell* 22: 508-522

Yeats, T.H. & Rose, J.K. 2013. The formation and function of plant cuticles. *Plant Physiology* 163: 5-20